

---

A Flotation and Ultrasonic Elution Model  
For Processing Carbon-Grit:  
Case of a Gold Mine

---

*4<sup>th</sup> Year Project submitted*

in partial fulfilment of the requirements for

The degree of  
**BSc Metallurgical Engineering**  
from

Department of Mining Chemical and Metallurgical Engineering  
Faculty of Engineering & the Built Environment

*by*

Primrose R. Mlambo

*under*

Eng S. B. Chinosengwa

UNIVERSITY OF ZIMBABWE

HARARE, ZIMBABWE

---

May 2023

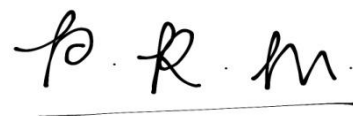
---

# Declaration of Authorship

**I**, Primrose R. Mlambo, hereby declare that the project entitled “*A Flotation and Ultrasonic Elution Model for Processing Carbon-Grit*” represents my own work, except where due acknowledgment has been made and that it has not been previously submitted for any other degree or diploma at any other institution. I also acknowledge any assistance or support that I have received during the research and writing of this dissertation. I have taken all necessary steps, to the best of my knowledge and understanding, to ensure that I properly acknowledged sources used in this research.

I declare that this dissertation conforms to the regulations and guidelines of the University of Zimbabwe and I am responsible for ensuring that the final manuscript is complete and accurate.

Date Submitted: 27 May 2023

Handwritten signature of Primrose R. Mlambo in black ink, consisting of the initials 'P. R. M.' with a horizontal line underneath.

.....  
Signature of Student

# Acknowledgements

---

I would like to thank all the individuals from different fields of Metallurgical Engineering and Mathematics, who provided invaluable advice and assistance during the course of this project.

I am deeply appreciative of Mr. T. Chikomo (Plant Metallurgist) and the staff at the CASE STUDY Plant, among them include the G.T's, Met Lab, Assay Lab, Mr. G. Mberekwa (Shift Co-ordinator), Mr. L. Mangava (Plant Superintendant), Mrs. C. Mundiya (Met Services Manager), Mr. E. Mudoti (Plant Manager), Mr. N. Mutaki (HR Business Partner), just to mention a few, for their immaterial mentorship and assistance during my attachment period February-December 2022.

Additionally, I extend my gratitude to my academic supervisors, Eng S. B. Chinosengwa, Eng T. Mubaiwa and the faculty members at the Department of Mining Chemical and Metallurgical Engineering for encouraging, nurturing and stretching my academic inquisition throughout my university career. I would also like to acknowledge the support and conducive environment extended by my fellow Metallurgical Engineering colleagues (Class of 2022-2023) during our learning period.

Above all, I give thanks to the Almighty God, the ultimate Author and Creator of everything. Without His grace and mercy, I would not have been able to achieve this milestone.

## *Dedication*

*To my mother and father –*

*Mavis and Canny,*

*for showing me the true meaning*

*of commitment and selflessness...*

# Abstract

---

This project focuses on the concentration and elution of loaded carbon and carbon fines from grit for the recovery of gold using froth flotation and ultrasonic elution techniques. The best collector-frother reagent combination used was found to be 6ml Kerosene and 6ml Waste Bio-Oil, while the optimum size fraction for froth flotation was  $-75\mu\text{m}$ . The ultrasonic elution process was simulated using DWSIM, achieving steady-state conditions at  $84^{\circ}\text{C}$ ,  $101\text{kPa}$  and  $44\text{kg/h}$ . The elution efficiency achieved, based on molar flow, was 51.2%. Mathematical process models were developed to observe the kinetics of elution; monitoring how the rate of gold concentration in eluant varies over time when the elution process is no longer homogeneous due to changes in particle size distribution, the elution process is no longer at steady-state due to a change in flow regime or ultrasonic frequency. The results of this study provide valuable insights into the effective handling and processing of carbon-grit for the recovery of gold, which, subsequent to conducting pilot plant studies, may prove useful in the design of future gold recovery processes.

# Abbreviations & Acronyms

---

GOLD MINE – Case Study mine

ROM – Run of Mine

SAG – Semi-Autogenous Grinding

CIP/CIL – Carbon in Pulp/Carbon in Leach

MKN screens – cylindrical screens of 850µm aperture

AARL – Anglo American Research Laboratory process

GLCF – Gold Loaded Carbon Fines/loaded carbon

CIL 1 and CIL 2 – Case Study processing Plant 1 and processing Plant 2

DZT545 – Betamin DZT545

D – Diesel

K – Kerosene

S – Sodium isopropyl xanthate/SIPX

WBO – Waste bio-oil

C-F – Collector-Frother combination

# Key Definitions

---

- 1.** Raw carbon-grit sample – constituted by size fractions 2.80mm, 2.00mm, 1.70 mm, 1.18 mm, 850 $\mu$ m and -850 $\mu$ m.
- 2.** Sample A – basket term for raw carbon-grit of larger individual size fractions of 2.00mm, 1.70 mm and 1.18 mm, which were used as feed input into froth flotation process.
- 3.** Sample B – basket term for raw carbon-grit of smaller individual size fractions of 850 $\mu$ m, 75 $\mu$ m, 53 $\mu$ m, which were used as feed input into froth flotation process.
- 4.** Froth A – a well mixed sample aggregate of all the froth concentrates obtained from froth flotation of Sample A size fractions.
- 5.** Froth B – a well mixed sample aggregate of all the froth concentrates obtained from froth flotation of Sample B size fractions.

## Table of Contents

Declaration of Authorship .....	i
Acknowledgements .....	ii
<i>Dedication</i> .....	iii
Abstract .....	iv
Abbreviations & Acronyms .....	v
Key Definitions .....	xii
List of Figures .....	xviii
List of Tables.....	xviii
List of Symbols .....	xix
CHAPTER ONE: INTRODUCTION.....	1
1.0 Background.....	1
1.1 Process Flow .....	2
1.1.1 Comminution, Classification & Leaching .....	2
1.1.2 Adsorption, Elution & Smelting .....	4
1.1.3 Carbon Management.....	5
1.2 Project Statement .....	7
1.3 Project Aim.....	8
1.4 Research Objectives.....	8
1.5 Project Justification.....	8
CHAPTER TWO: LITERATURE REVIEW .....	10
2.0 Introduction .....	10
2.1 Coal & Activated Carbon .....	10
2.1.1 Surface Properties of Coal .....	10
2.2 Activated Carbon in Gold Processing .....	11
2.2.1 Adsorption .....	11
2.2.2 Elution.....	11
2.2.3 AARL Elution Method.....	12
2.2.3.1 AARL Elution Efficiency & Particle Size Distribution.....	12
2.3.0 Generation of Loaded Carbon Fines in Gold Processing .....	13
2.3.1 General Abrasion .....	13
2.3.2 Impeller Motion in CIP/CIL Tanks.....	13
2.3.3 Carbon Regeneration .....	13

2.3.4 Poor Carbon Management.....	14
2.3.5 Poor Classification.....	14
2.4 Treating Loaded Carbon Fines for Gold Recovery .....	14
2.4.1 Case Study .....	14
2.4.1.1 Separation of Loaded Carbon Fines from Grit.....	14
2.4.1.2 Storing Loaded Carbon Fines.....	15
2.4.2 Conventional Methods.....	15
2.4.2.1 Agglomeration .....	15
2.4.2.2 Sintering.....	15
2.4.2.3 Oil Agglomeration.....	16
2.4.2.2 Direct Froth Flotation .....	16
2.4.2.3 Carbon Ashing.....	19
2.4.2.4 Ultrasonic Elution Method .....	19
2.4.2.5 Waste Material .....	20
2.5 Economic Benefit from Processing Loaded Carbon Fines for Gold Recovery .....	20
2.6 Environmental Considerations in Processing Loaded Carbon Fines .....	21
2.6.1 Froth Flotation .....	21
2.6.2 Ultrasonic Elution .....	21
2.7 Digitisation in Processing Loaded Carbon Fines.....	22
2.7.1 Froth Flotation .....	22
2.7.2 Ultrasonic Elution .....	23
2.8 Simulation .....	24
2.8.1 Ultrasonic Elution Simulation using DWSIM .....	24
2.8.2 DWSIM & METSIM .....	24
2.9 Mathematical Modeling.....	25
2.9.1 Benefits of using Mathematical Modeling .....	25
2.9.2 Solving ODEs using Numerical Solutions .....	25
2.9.3 Other Types of Mathematical Models.....	26
CHAPTER THREE: METHODOLOGY.....	28
3.0 PPE.....	28
3.1 Sample Collection using Systematic Random Sampling.....	28
3.1.1 Apparatus:.....	28
3.1.2 Reagents & Materials.....	28
3.1.3 Procedure.....	28

3.2 Composite Head Assay using Fire Assay Method.....	29
Quantifying Au, Ag and Cu adsorbed onto activated carbon.....	29
3.2.1 Apparatus .....	29
3.2.2 Reagents & Materials .....	29
3.2.3 Procedure .....	29
3.3 Particle Size Distribution (PSD) of Raw Carbon-Grit .....	30
PSD was conducted as part of characterizing raw carbon-grit sample.....	30
3.3.1. Apparatus .....	30
3.3.2. Reagents & Materials .....	30
3.3.3. Procedure .....	30
3.4 Abrasion Test of Carbon-Grit.....	31
Abrasion Test was conducted as part of characterizing carbon-grit sample. ....	31
3.4.1. Apparatus .....	31
3.4.2. Reagents & Materials .....	31
3.4.3. Procedure .....	31
3.5 Preparation of Sample A.....	32
3.5.1 Apparatus .....	32
3.5.2 Reagents & Materials .....	32
3.5.3 Procedure .....	32
3.6 Preparation of Sample B.....	33
3.6.1 Milling Carbon-Grit Mixture.....	33
The carbon-grit sample was homogenized in size through implementing a grinding stage. ....	33
3.6.1.1 Apparatus.....	33
3.6.1.2 Reagents & Materials.....	33
3.6.1.3 Procedure .....	33
3.6.2 Preparation of Sample B .....	34
3.6.2.1 Apparatus .....	34
3.6.2.2 Reagents & Materials .....	34
3.6.2.3 Procedure.....	34
3.7 Specific Gravity (SG) Test of Sample A & Sample B.....	35
SG Test was conducted as part of characterizing Sample A and Sample B. ....	35
3.7.1 Apparatus.....	35
3.7.2 Reagents & Materials .....	35

3.7.3 Procedure .....	35
3.8 Concentrating Carbon through direct Froth Flotation .....	35
3.8.1. Apparatus .....	36
3.8.2 Reagents & Materials .....	36
3.8.3 Procedure .....	36
(a) Sample A (size fractions 2.00mm, 1.70mm and 1.18mm): .....	36
(b) Sample B (size fractions 850µm, 75µm and 53µm): .....	38
3.9 Ultrasonic Elution of Carbon Froth Concentrate .....	38
3.9.1 Apparatus .....	38
3.9.2 Reagents & Materials .....	38
3.9.3 Simulation Procedure .....	39
1. Simulation Model.....	39
2. Simulation Objectives.....	39
3. Input Parameters .....	39
4. Simulation Process Flowsheet .....	40
5. Output Metrics .....	40
6. Experimental Design .....	40
7. Assumptions & Limitations.....	40
8. Validation & Verification .....	41
CHAPTER FOUR: RESULTS & DISCUSSION .....	43
4.0 Introduction .....	43
4.1 Characterisation Results .....	43
4.1.1 Particle Size Distribution & Gold Department Analysis .....	43
4.1.1.1 Raw Carbon Grit Sample Analysis.....	44
4.1.1.2 Sample A & Sample B Analysis.....	45
4.1.2 Effect of Physical Properties of Sample A & Sample B .....	47
4.1.2.1 Specific Gravity Analysis.....	47
4.1.2.2 Abrasion Test Analysis.....	48
4.2 Froth flotation for Carbon-Grit Separation .....	49
4.2.1 Effect of Size Fraction on Mass Pull.....	50
4.2.1.1 Statistical Model Analysis .....	51
4.2.2 Effect of Collector-Frother Combination on Mass Pull.....	52
4.2.3 Effect of Froth Flotation on Gold Department .....	53
4.3 Ultrasonic Elution of Loaded Carbon Concentrate .....	54

4.3.1 Steady-State & Elution Efficiency.....	55
4.3.2 Mathematical Model Analyses of Ultrasonic Elution.....	56
1. Steady-State Model .....	58
2. Non-Homogenous Model.....	61
Effect of Particle Size with Changes in $e_{(aq)}[Au]$ over Time.....	61
3. Non Steady-State Model .....	62
Effect of Varying Flowrate on $e_{(aq)}Au$ over Time.....	62
4. Non Steady-State Model .....	64
Effect of Varying Frequency on $e_{(aq)}Au$ over Time.....	64
CHAPTER FIVE: CONCLUSION AND RECOMMENDATIONS .....	65
5.0 Introduction .....	65
5.1 Conclusions .....	65
5.2 Recommendations .....	66
Bibliography.....	68
Appendices.....	73
Appendix A: Characterisation Results.....	73
Appendix B: Froth Flotation Results .....	75
Appendix C: Ultrasonic Elution Simulation Data Set .....	77
Appendix D: File Resources .....	80

# List of Figures

Figure 1: Geological map of the Bindura– Shamva greenstone belt and surrounding granitoid–gneiss terranes (Jelsma & Dirks, 2000) .....	1
Figure 2: Mineral processing flowsheet (Case Study, 2022). .....	3
Figure 3: CIP/CIL circuit (Case Study, 2022).....	6
Figure 4: Historic gold production (Case Study, 2020). .....	7
Figure 5: Mechanisms of particle-bubble interaction (Sokolović, J.; Mišković, S., 2018).....	17
Figure 6: Principle of ultrasonic cavitation (Industrial Quick Search).....	20
Figure 7: Overview map illustrating coal mining concessions and protected natural reserves in the Hwange District, Western Zimbabwe (2018). .....	22
Figure 8: Ultrasonic elution schematic (Feng, D. et all, 2002). .....	40
Figure 9: PSD and gold deportment of raw carbon-grit sample. ....	44
Figure 10: Sample A size fraction, 2.00mm. ....	45
Figure 11: Sample A size fraction, 1.70mm.....	45
Figure 12: Sample A size fraction, 1.18mm. ....	45
Figure 13: PSD and gold deportment of Sample A and Sample B. ....	46
Figure 14: Assay analysis of Sample A and Sample B.....	47
Figure 15: SG analysis of Sample A and Sample B.....	48
Figure 16: Abrasion analysis of Sample A and Sample B. ....	49
Figure 17: Froth flotation efficiency.....	51
Figure 18: C-F performance per reagent combination basis. ....	52
Figure 19 Effect of froth flotation on gold deportment .....	53
Figure 20: Ultrasonic simulation flowsheet in DWSIM.....	55

# List of Tables

Table 1 showing volumes added per single run through of flotation test procedure ..	37
Table 2 C-F Combination Identities .....	50
Table 3: Expected Gold Content from processing loaded carbon .....	55

# List of Symbols

$M_{c,i}$  = initial mass of carbon

$M_{c,v}$  = final mass of carbon

$C_{c,i}$  = initial gold concentration on carbon

$C_{c,v}$  = final gold concentration on carbon

$M_{e,i}$  = initial mass of eluant

$M_{e,v}$  = final mass of eluant

P = ultrasonic bath

f = ultrasonic wave frequency

A ~ ultrasonic wave amplitude

$c_{p,e}$   $\approx$  specific heat capacity of eluant

$e_{(s)}[\text{Au}]$  = gold concentration in eluant

$C_{(s)}[\text{Au}]$  = gold concentration in loaded carbon

## CHAPTER ONE: INTRODUCTION

This chapter introduces the research by giving an elaboration of the project highlights, which include background of CASE STUDY mine, problem statement, aim, objectives and justification.

### 1.0 Background

GOLD MINE is situated in Bindura, Zimbabwe and its gold deposits<sup>1</sup> are located on the upper part of the Bindura plateau on the southwestern margins of the intrusion. The GOLD MINE processes low-grade gold ore into bullion and sells to the official gold refinery and buyer at the prevailing gold price.

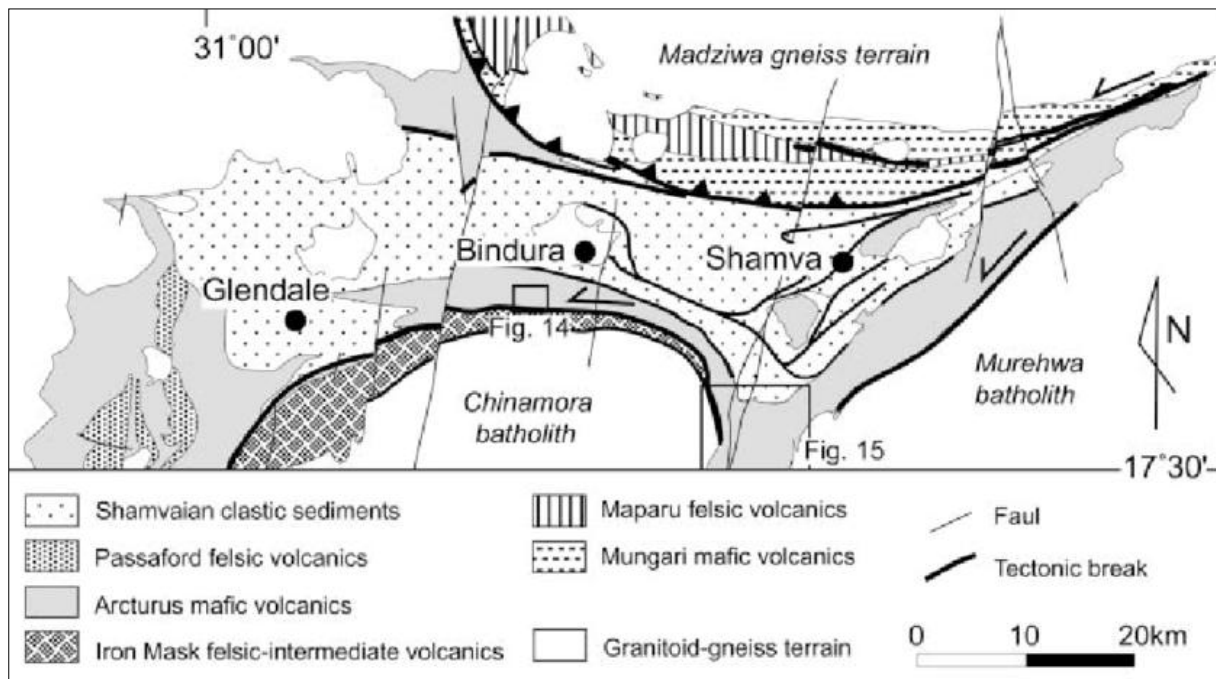


Figure 1: Geological map of the Bindura–Shamva greenstone belt and surrounding granitoid–gneiss terranes (Jelsma & Dirks, 2000).

GOLD MINE started its operations in 1985 under the ownership of Ashanti Goldfields, on discovery of oxide and sulphide gold deposits. In the same year, mining production commenced via two open pit mines under Cluff Resources (Pvt) Ltd. A year passed and the GOLD MINE witnessed its first gold pour. Underground

<sup>1</sup> Figure 1. Jelsma & Dirks (2020). A tectonic origin for ironstone horizons in the Zimbabwe craton and their significance for greenstone belt geology. *Journal of the Geological Society*. 160(1). p. 83-97.

mining was initiated shortly after ownership was passed onto Ashanti Goldfields Zimbabwe (Pvt) Ltd, which later became known as Anglo-Gold Ashanti in 1996. Over time, the open pit resource experienced depletion. This saw yet another change of ownership – where this time, Mwana Africa (Pvt) Ltd came to full acquisition of the mine in 2004. Early 2020 saw the Mine asset shift hands into its current ownership – Kuvimba Mining House, which, according to (Hove, 2021) broke a 20-year production record as it produced 300kg worth of bullion in June 2021 alone.

Publicly released financial data to-date show GOLD MINE to be among some of the largest registered large-scale gold producers in Zimbabwe, reporting a gold output production rate of 3t per annum at an average built-up head grade of 1.39g/t.

## **1.1 Process Flow**

GOLD MINE obtains its run-of-mine (ROM) from an open pit mine and an underground mine at an average head grade of 1.40g/t. Successive comminution and classification take place and result in the processing of size-reduced ore through traditional Carbon in Pulp (CIP) and Carbon in Leach (CIL) methods. The elution process ensues the CIP/CIL process, followed by smelting of a gold-rich sludge obtained from the electrowinning process. The final semi-finished product(s) are minimum 600ppt Au fineness bullion bars<sup>2</sup>.

### **1.1.1 Comminution, Classification & Leaching**

A live stockpile at the Main Plant is fed by two primary crushers - one 42 X 48 and one 50 X 60 Telsmith jaw crusher, which reduce ROM to manageable proportions. Secondary crushing is enabled by one 21inch Symmons hydrocone crusher, which is placed in series to the primary crushing circuit. Upon reduction to size, the ore is finally conveyed to the livestock pile for intermediary storage, as constant feed input is required for continuous operation of the milling section. The ore is ground and classified through Semi-Autogenous (SAG) mills, hydrocyclones and dewatering cluster cyclones. Knelson centrifugal gravity concentrators are found between the mill discharge and primary cyclones, in order to concentrate gravity-recoverable gold and perform intensive cyanidation of material, in the In-Line Leach Reactor, using

---

<sup>2</sup> Figure 2. Case Study (2022). Mineral processing flowsheet.

20L of hydrogen peroxide and a 10,000ppm cyanide concentration. Almost 20% of gold is recovered through this method.

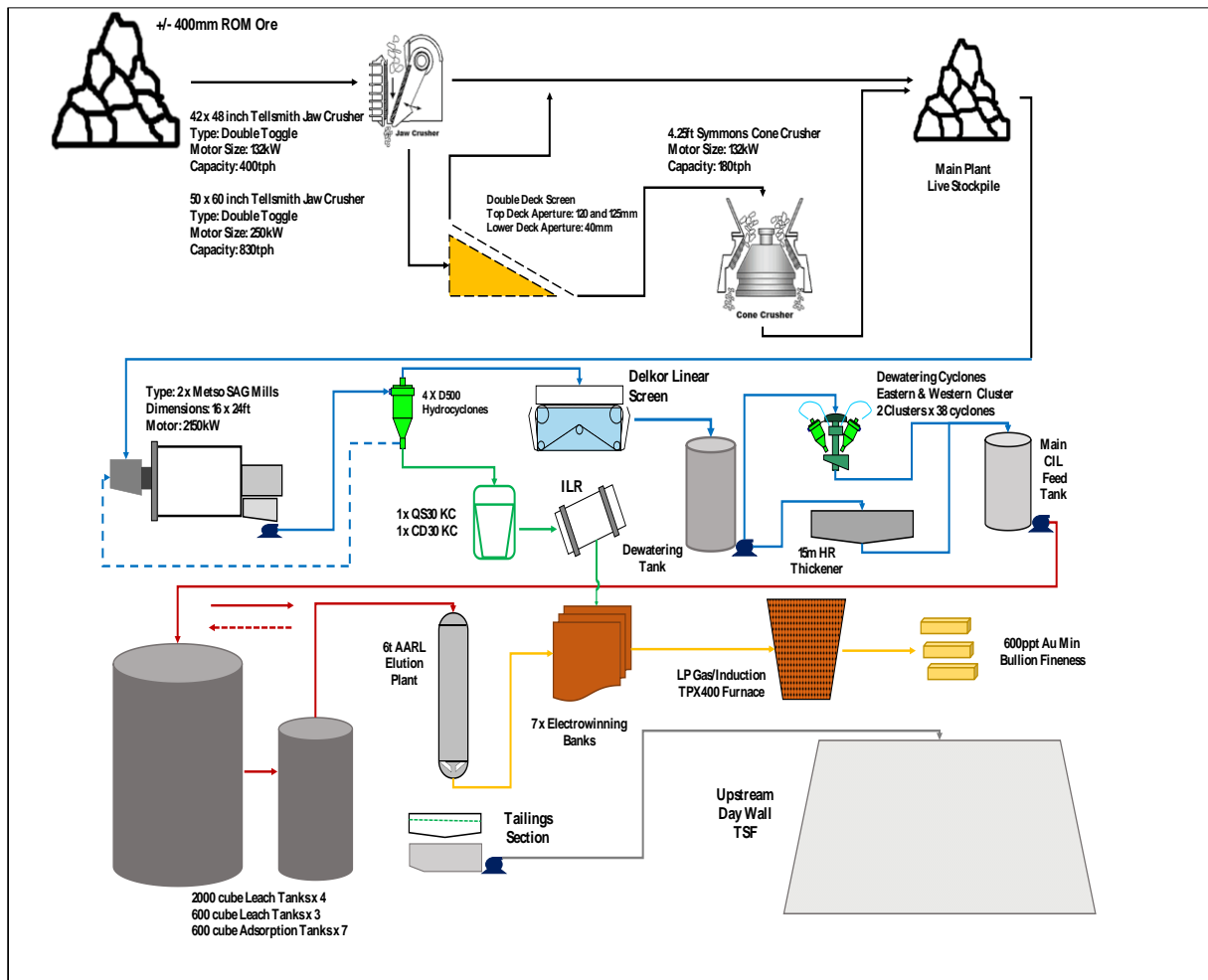
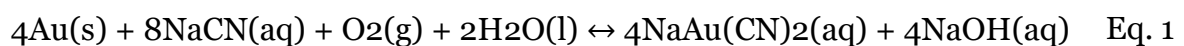


Figure 2: Mineral processing flowsheet (Case Study, 2022).

A thickener uses flocculant to improve the density and grind of the dewatering cyclone overflow. The product from the agglomeration becomes the input into the CIP/CIL tanks. GOLD MINE uses cyanide as its leaching agent in the CIP/CIL circuit with a concentration range of 300-450ppm. Cyanide plays an important role as it selectively leaches out chemically bound gold into solution, along with other base metals. Lime, oxygen and water are added to the pulp in adequate amounts to optimize the leaching tanks' reaction kinetics, based on Elsner's equation<sup>3</sup>:



<sup>3</sup> Elsner's equation describes the process of gold leaching using cyanide as a leaching agent.

For the optimization of leaching and subsequent carbon adsorption, reagent dosages and physical plant parameters are closely controlled and manually monitored for maximum gold dissolution into solution e.g. pulp density, tank depths, grind, carbon concentration, only to name a few. The movement of the agitators (with a double impeller system) in all 13 leaching and CIP/CIL tanks (connected in series) facilitates mixing motion in-between pulp and reagents, enabling optimum collision time on a wider surface area for the success of the leaching and adsorption reactions. The pulp will therefore have a total residence time which averages 28-35hrs travelling from Tk0 to Tk13.

### **1.1.2 Adsorption, Elution & Smelting**

Activated carbon is used as a gold adsorbent and it is added to Tk13 (last tank) in the CIP/CIL circuit. The activated carbon is moved counter-current against the pulp through the use of Salor pumps and MKN screens of aperture 850 $\mu$ m. Activated carbon adsorbs calcium gold aurocyanide, a non-polar compound, onto its internal porous structures at an optimum gold loading of 5,000g per tonne of activated carbon added. (Rogans, n.d.)

At the header tank (Tk7), gold loaded carbon is extracted, screened, washed and eluted in Anglo American Research Laboratory (AARL) process parameters. AARL elution is a batch process which incorporates acid washing and elution of the gold loaded carbon in a single elution column, at a temperature of 127°C and a pressure of 300kPa. The gold loaded carbon forms the stationary phase and is placed in contact with the eluant solution of caustic soda (NaOH), which forms the mobile phase. The gold is de-adsorbed from the carbon pores and redissolves into solution to form the eluate solution. This process runs for a duration of 4 to 6 hour intervals.

After elution, the eluate/electrolyte is passed through the electrowinning process. The process of electrowinning requires the use of grade 0 steel wire wool, primarily made of iron. An acid digestion step succeeds electrowinning, as the electroplated wire wool cathodes are mixed with either hydrochloric acid (HCl), nitric acid (HNO<sub>3</sub>) or aqua regia. The resultant gold-rich sludge is decanted, dried and calcined over a liquefied petroleum (LP) gas-fired furnace.

Fluxes are added to the dry calcine, in the following ratios – 40% borax, 25% sodium nitrate, 25% silica and 5% fluorspar. These flux ratios impart desirable chemical and physical properties to the slag that lower its melting point, ensure unwanted base metals are oxidized, neutralize the base metal oxides formed in order to protect crucible lining and overall impart good slag viscosity. This forms the final furnace charge which is smelted at 1,200 °C for 1h.

The molten metal is tactfully poured from the furnace opening and into pre-heated moulds. The moulds are rapidly cooled to form solid “yellow” bullion bars. Each bullion bar is given an identity and proceeds for drilling stage. Drilling is used to obtain samples of minimum weight 5g that will be assayed for gold and silver fineness and content. The final mass of each bullion bar is weighed and logged into the online “Fidelity Printers” bullion data tracking application.

### **1.1.3 Carbon Management**

Carbon sizes of <math>-3\text{mm}</math> are classified as carbon fines and ultrafines. Gold Loaded Carbon Fines (GLCF) emanate from abrasion, attrition and overall wear of activated carbon in the CIP/CIL tanks<sup>4</sup>. As carbon moves counter-current from Tk 13 to the header tank, its size wears down from +3mm to -3mm; this carbon size cannot be eluted due to stripping inefficiencies in the AARL parameters. GLCF permeate through the following: 850µm MKN screen apertures in CIP/CIL tanks, 850µm carbon screening decks and wedge wire screen filters sized US MESH 3-4 (6.73-4.76 mm) in the elution column. GLCF also emanate from the Carbon Regeneration process. Rapid cooling of carbon releases fines which contain decent gold loadings as remainders from the elution process.

---

<sup>4</sup> Figure 3. Case Study (2022). CIP/CIL circuit.

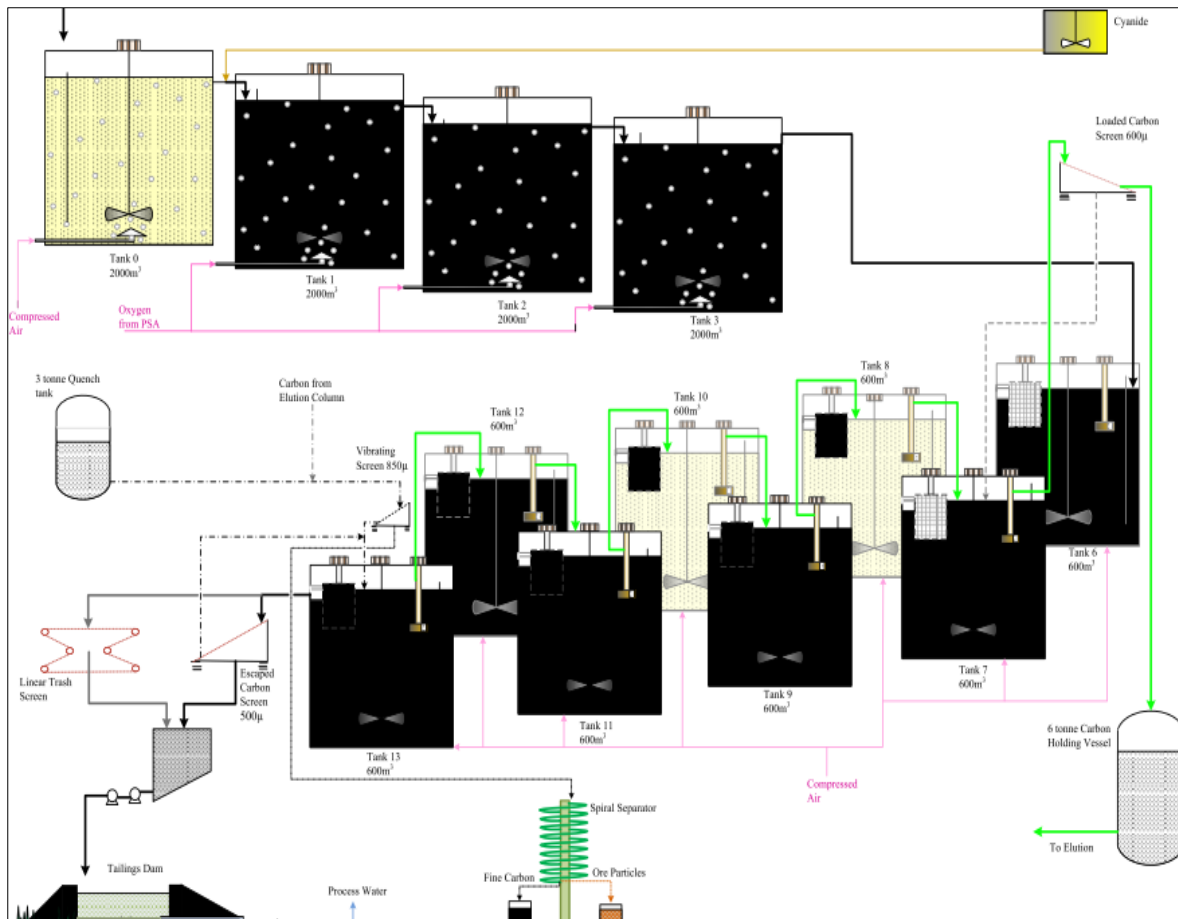


Figure 3: CIP/CIL circuit (Case Study, 2022).

Trend shown by figure 4 below, suggests that within the context of GLCF, gold lockup resulting from not processing GLCF has been causing an observable disparity between actual gold recovery and budget gold recovery, tracked over a period of 10 years. Within the context of gold mineral processing, the generation of GLCF is inevitable within CIP/CIL based operations. GLCF are regarded as waste material with little to no immediate economic value but contrary to public opinion, the researcher proposes that value could be salvaged from GLCF, resulting in significant ecological and financial benefits for gold processing organizations such as at the CASE STUDY and local gold mines in general.

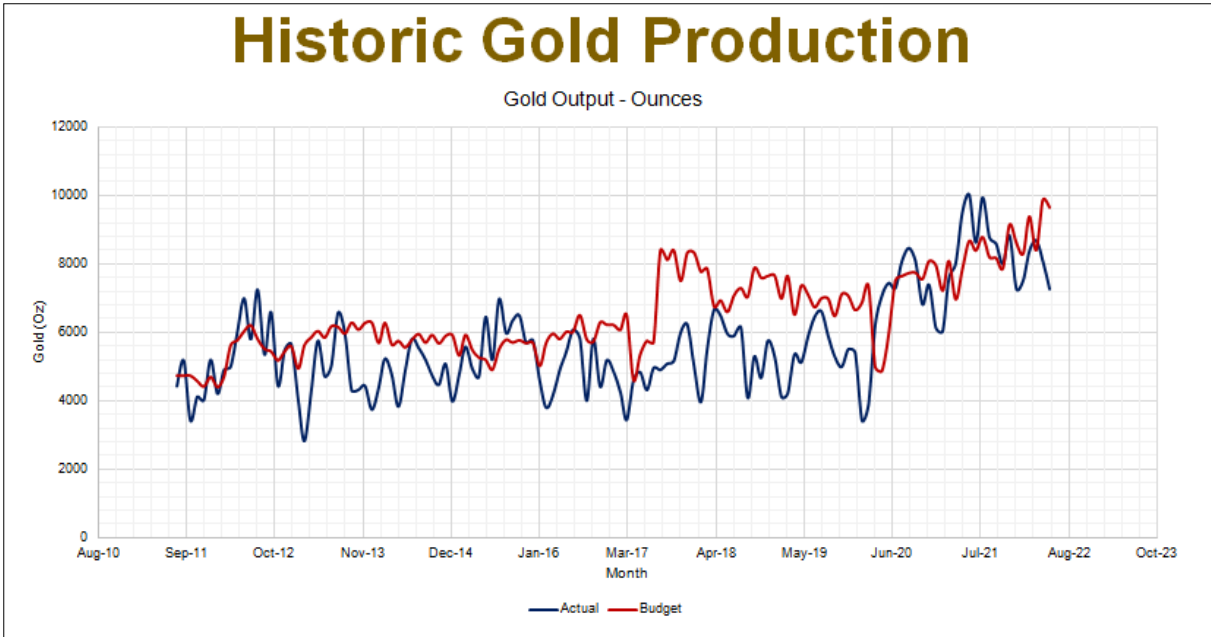


Figure 4: Historic gold production (Case Study, 2020).

### 1.2 Project Statement

GOLD MINE is facing a dichotomy concerning the ineffective handling and processing of GLCF. The current method of separating loaded carbon/GLCF from grit is proving inefficient and GOLD MINE is facing the problem of a growing carbon-grit inventory, which reduces the overall expected gold output on a monthly basis by 3-5kg. As shown in Appendix A-1, a Wilfley Shaking Table is presently in operation, for the purpose of carbon-grit separation; however, it is operating at a capacity of 6.00t per month against a monthly GLCF generation of 7.90t. This is further adding to a 72t dormant carbon-grit inventory currently held to-date.

GOLD MINE is running an average of 42 elution cycles per month. Upon concentrating the 72t inventory plus monthly generated GLCF hereon after, it would require an additional 12 elution cycles, which would result in a backlog of elutions as the plant cannot afford to stop downstream processes in order to cater for these reoccurring batches. AARL operating pressure of 300kPa does not allow for functional and practical elution of GLCF due to the nature of the small carbon particles. Elution productivity is closely associated with laminar flow of eluant inside the elution column. Laminar flow is particularly favoured by a large and coarse Particle Size Distribution, therefore, the partial accumulation and resultant blinding

of the filters and screens at the bottom of the elution column deem processing of GLCF unworkable.

Therefore, CASE STUDY is missing out on an opportunity cost through the recovery of gold trapped in the loaded carbon fines, which is by and large of major economic benefit to the mine's profit generating activities.

### **1.3 Project Aim**

To develop a froth flotation and ultrasonic elution model for the concentration and elution of gold loaded carbon fines at GOLD MINE and recommend its use as an integrated plant process, in increasing monthly gold output.

### **1.4 Research Objectives**

- 1) To carry out an extensive characterisation of the carbon-grit mixture.
- 2) To investigate the use of direct froth flotation on the carbon-grit sample in order to obtain a carbon concentrate.
- 3) To design, simulate and mathematically model the kinetics of an ultrasonic elution bath model for the recovery of gold from carbon concentrate.

### **1.5 Project Justification**

Given the absence of an effective long-term strategy that addresses the problem, GLCF are left to growing stockpiles. By undertaking this project, the following benefits can be derived:

#### **1. Increase in Revenue from Inventory**

At an average composite head grade of 300g/t, GOLD MINE is holding a 72t inventory of GLCF mixed with grit stored in 210L drums and live stockpiles. Average gold price (as at January 25, 2023) is US\$1,926.46/oz. This means that GOLD MINE can realize approximately US\$1,426,967.00 in gold sales revenue.

#### **2. Increase in Revenue Annually**

The generation of carbon fines in the CIP/CIL circuit is inevitable. GOLD MINE uses Donau 6X12 activated carbon which has an abrasion rate of 3.7%. Therefore, for

every 1t of activated carbon added to the CIL/CIP tanks, ±37kg forms GLCF. This translates to ±US\$160,564.59 in reoccurring sales revenue.

Tank sanding is a reoccurring problem at GOLD MINE and requires that the tanks be drained. It is approximated that tanks sand at a rate of 1Tk/month due to sudden power cuts which cause turbines to momentarily shutdown, resulting in carbon, pulp and solution to segregate and settle. GLCF drained from any one sanded tank constitute approximately 1.71t of the total mass of pulp in a tank, which can markedly augment to gold output per month.

### **3. New Potential Revenue Stream**

An untapped market of 50,000 registered small-scale gold miners exists in Zimbabwe, who by and large treat their GLCF as waste due to lack of access to effective processing systems. Therefore, GOLD MINE is presented with an investment opportunity of purchasing and processing GLCF from other gold mines for the recovery of gold trapped in the carbon fines. This is an efficacious business strategy of sustainable economic benefit to the GOLD MINE, as the market is still under saturated.

### **4. Removal of Storage Footprint**

A high carbon storage footprint is associated with poor housekeeping standards. The salvage yards are not wind-proofed to inhibit strong winds from dispersing dust and contributing to air pollution. The inhalation of dust is detrimental to the health of the workers. Long-term exposure to dust inhalation has been shown to promote the development of pneumoconiosis. Therefore, Safety, Health and Environment (SHE) considerations will be addressed in the processing of carbon-grit stockpiles.

Another point of concern often overlooked at the Plant is the apparent security risk posed by GLCF stock yards. The ease of access to the carbon-grit salvage yard poses a high probability of undetectable theft due to the nature of the GLCF, which are small in size, hence cannot be picked up by the metal detectors.

## **CHAPTER TWO: LITERATURE REVIEW**

### **2.0 Introduction**

This literature review aims to establish a solid framework for the current study of concentrating and eluting gold loaded carbon fines. The review follows sequential logic, drawing on various sources of information including peer-reviewed journal articles, textbooks, periodicals and other relevant sources of information, in order to enhance the validity of the findings.

### **2.1 Coal & Activated Carbon**

Coal is a naturally occurring rock with varying impurities, while activated carbon is a synthetic spongy material with numerous interlocking pores and it cannot be represented by a molecular formula or qualitative analysis. It is produced by dry distilling carbonaceous material at high temperatures. The carbonaceous material used for activated carbon production can include coconut shells, wood and cellulose. (Hassler, 1974) defined activated carbon as a group of carbonaceous materials with unique physical and chemical properties. Although coal and activated carbon are different forms of carbon, they exhibit similar chemical surface properties which can be extrapolated between the two to make approximate deductions (Rogans, 2012) (Marsden & House, 2006).

#### **2.1.1 Surface Properties of Coal**

As previously mentioned, activated carbon has similar chemical properties to carbon. Therefore, it is also inert, meaning it carries no charge on its outer or inner porous surface. As a result, activated carbon can only adsorb neutrally charged complexes from solution, making it a cheap and ideal adsorbent in the gold processing industry. The surface properties of coal, a material similar to activated carbon, depend on the hydrocarbon skeleton. The quantity and characteristics of oxygen functional groups and mineral matter impurities present in the coal sample can play a significant role in determining its surface properties and suitability for various applications, according to (Fuerstenau, 1983)'s characterisation of coal surface properties (Gupta, n.d.) (He & Laskowski, 1992). Flotation tests have been used in the coal industry to separate coal fines based on their hydrophobicity and similar tests can therefore be

derived for activated carbon flotation based on the chemical similarity between the two materials.

## **2.2 Activated Carbon in Gold Processing**

### **2.2.1 Adsorption**

Adsorption is the tendency of atoms or molecules in liquid or gas state to adhere to a solid surface, as defined by (Maitson & Mark, 1971). In gold processing, activated carbon acts as the solid surface that facilitates the adsorption of gold complexes. Due to the neutral surface charge, activated carbon can only adsorb neutral gold complexes. Cyanide is one of the few chemicals that can effectively react with gold and it selectively dissolves gold from its ore in the presence of lime, oxygen and water. The negatively charged gold cyanide ion reacts with positive ions such as calcium to form a neutral and relatively stable metal complex, which can then be adsorbed onto activated carbon.

### **2.2.2 Elution**

The desorption equilibria of calcium aurocyanide from loaded activated carbon has been described by linear isotherms, indicating that the adsorption process is thermodynamically reversible. Elution is the process of extracting an adsorbed material from an adsorbent, by washing it in a solvent. In gold processing, gold in the form of calcium aurocyanide is stripped from loaded carbon into an alkaline solution through elution. This is achieved via a chemical reaction that forms the eluate. Two widely used methods of elution are Anglo American Research Laboratory (AARL) process and Zadra process. In the AARL process, batch elution is performed over a period of 6-10 hours, while in the Zadra process, elution and electrowinning operate concurrently through a continuous in-series circulation of the eluate through the elution column and the electrowinning cells. These methods have been traditionally used in gold processing for their technical and economic advantages (Achaw & Danso-Boateng, 2021) (Habashi, 1999) (Habashi, 2015).

### **2.2.3 AARL Elution Method**

As a preliminary step to carbon regeneration, pregnant carbon is soaked in 1 bed volume (BV) of dilute hydrochloric acid (HCl) and then washed with 2 BVs of potable water in the acid wash column. This step can occur before or after elution. In the next step, the carbon is transferred to an elution column and is soaked with 1 BV of a caustic-cyanide solution at a temperature of 120°C for 30 minutes. The industry practice is to use 2.5% v NaOH and 3% v NaCN, but lower reagent concentrations have been observed to yield sufficient elution efficiencies. Loaded carbon is then eluted at 127°C, 300kPa, for 6-8 hours. Loaded carbon forms the stationary phase while the eluant forms the mobile phase. Calcium aurorocyanide desorbs into the moving eluant stream and solution obtained can be passed through electrowinning on concluding the elution cycle. Based on plant observations, the negation of NaCN does not appear to have any negative effects on operational efficiencies.

#### **2.2.3.1 AARL Elution Efficiency & Particle Size Distribution**

Carbon fines with a narrower particle size distribution tend to have a higher adsorption capacity for gold and other metals, as compared to those with a wider particle size distribution. However, they can also be more difficult to elute due to the increased likelihood of particle-to-particle contact, which can result in the formation of agglomerates and hinder the flow of the eluting solution through the bed of carbon particles. On the other hand, carbon fines with a wider particle size distribution may have a lower adsorption capacity but can be more easily eluted due to their increased porosity and permeability, which allows for more efficient contact with the eluting solution (Rao, et al., 2008).

However, it is worth noting that the optimal particle size distribution for elution may depend on the specific conditions of the process, such as the type of carbon fines and the pressure or flowrate at which eluant is in circulation (Fleming & Cromberge, 1984). Optimizing elution parameters for carbon fines with a narrow particle size distribution involves finding a balance between maximizing the elution of adsorbed metals and minimizing the risk of agglomeration and channelling (Rao, et al., 2008).

### **2.3.0 Generation of Loaded Carbon Fines in Gold Processing**

Activated carbon fines in the gold processing circuit can be considered to emanate from the following:

1. General Abrasion
2. Impeller Motion in CIP/CIL Tanks
3. Carbon Regeneration
4. Poor Carbon Management
5. Poor Classification

#### **2.3.1 General Abrasion**

General wear caused by abrasion and attrition between pulp and activated carbon can lead to gold and carbon losses in carbon adsorption processes like CIP and CIL. According to (Van Dam, 1994), gold adsorption mainly occurs in the outer shell of activated carbon particles. Therefore, attrition fines have a higher gold concentration, as they pass through small apertures in carbon screens and spend more time in the CIP/CIL circuit adsorbing gold. It is therefore essential to minimize wear and tear between the pulp and activated carbon to reduce gold and carbon losses. This can be achieved through proper equipment design and optimizing operating conditions.

#### **2.3.2 Impeller Motion in CIP/CIL Tanks**

(Coetzee & Cloete, 1998) conducted a study that demonstrated how various types of impellers have different levels of abrasion impact on activated carbon. Turbines are typically installed to ensure homogenous mixing between reagents and pulp for effective leaching and adsorption kinetics. However, these turbines can also participate in direct attrition to activated carbon in solution, which can generate loaded carbon fines.

#### **2.3.3 Carbon Regeneration**

(Strudgeon & al., 1980) observed that post-elution barren carbon loses its adsorptive capacity and requires a regeneration process to ensure process sustainability. The regeneration system typically involves high temperatures of about 815-918°C and

subsequent quenching of the hot carbon using water can promote the generation of fines.

#### **2.3.4 Poor Carbon Management**

(Rowe & McKnight, 2009) explained that carbon losses can occur due to screen leakage and abrasion forces result from having too much carbon in any one tank at any one instance. Simply, poor carbon management in adsorption tanks promotes the production of loaded fines. These carbon fines can escape the CIP/CIL circuit and end up in the tailings section. (Van Dam, 1994) supported this idea, stating that carbon fines have a relatively high gold content. If left untreated, more and more gold locked up in carbon fines can accumulate, making the process uneconomical in the long run.

#### **2.3.5 Poor Classification**

Based on observations of manually run plant operations, poor grinds obtained during size reduction and classification can result in poor downstream parameters. When pulp enters the CIP/CIL tanks, poor grinds can affect the density, which is sensitive to efficient mixing and carbon adsorption. This can lead to sanding in the tanks, as there is insufficient liquid-solid ratio to maintain the pulp in suspension. Once the tanks become sanded, they are drained and loaded carbon fines inevitably end up in the tailings section. (FRGM, n.d.)

### **2.4 Treating Loaded Carbon Fines for Gold Recovery**

#### **2.4.1 Case Study**

##### **2.4.1.1 Separation of Loaded Carbon Fines from Grit**

GOLD MINE utilises a Wilfley shaking table, a mechanical method used to separate grit from loaded carbon fines. Shaking tables are used to separate particles based on their density, size and shape. The table uses a thin-film concentration process that progressively removes particles from top to bottom. The deck of the table moves asymmetrically, which helps to separate the particles in the longitudinal direction of the deck. One of the main features of shaking tables are riffles on the deck which

increase turbulence in the bottom portion of the thin-film flow, assisting in the transport of settled heavy particles towards the heavy product end and vertical plane stratification (Sivamohan & Forssberg, 1985).

In many coal cleaning plants worldwide, additional cleaning methods are utilized to meet specific requirements, such as low specific gravities or fine particle sizes. Jigs and shaking tables have demonstrated high efficiency in the specific gravity range of 1.50/1.60 to 1.80/1.90, whereas heavy media equipment is required for efficient separation at specific gravities of 1.40 or lower, depending on the particle size (Tiernon, 1973) (Zimmerman, 1981) (Zimmerman, 1982)

#### **2.4.1.2 Storing Loaded Carbon Fines**

GOLD MINE took to storing their processed gold loaded carbon fines. Storing loaded carbon fines for a prolonged period of time and in large quantities, poses environmental risk. Loaded carbon containing cyanide or heavy metals in deleterious amounts can release harmful pollutants into ground water sources and rivers. Carbon footprint associated with the transportation and storage of loaded carbon fines can have a distinct correlation with the organization's greenhouse gas emissions, which eventually lead to global warming. Security risk associated with carbon-grit salvage yards is that unauthorised access could potentially attract theft and vandalism. (Hilson & Murck, 2007)

#### **2.4.2 Conventional Methods**

##### **2.4.2.1 Agglomeration**

Agglomeration is a process used to concentrate carbon fines from grit by forming larger agglomerates that can be more easily separated from the grit. There are several types of agglomeration techniques that can be used to separate carbon fines from grit - sintering and oil agglomeration.

##### **2.4.2.2 Sintering**

Sintering is a high-temperature process that involves heating the carbon fines to a temperature below their melting point but above their re-crystallization temperature. This causes the particles to bond together and form larger agglomerates. Sintering

can be an effective method for producing agglomerates with a narrow size distribution and high strength, but it requires high temperatures and can result in the loss of volatile matter and organic compounds.

#### **2.4.2.3 Oil Agglomeration**

Oil agglomeration is when a hydrophobic reagent e.g. a collector is added to the carbon-grit mixture. Coalescence is resultant of the oil fully coating the non-polar carbon particle surface, causing agglomeration. The agglomerates can then be separated from the grit using flotation or sedimentation. Oil agglomeration can be an effective method for producing agglomerates with a high degree of selectivity and low ash content, but it requires careful control of the reagent dosage and can result in the loss of valuable hydrocarbons (Zhang & Wang, 2019) (Sun & Pan, 2018).

#### **2.4.2.2 Direct Froth Flotation**

Froth flotation is a commonly used method for separating carbon fines from other materials. The process involves adding a flotation reagent to the slurry of carbon fines which renders the carbon hydrophobic. Air bubbles are then introduced into the slurry and the hydrophobic carbon particles attach themselves to the bubbles and float to the surface, where they form a froth layer that can be collected and separated from the rest of the slurry. The process is effective for separating carbon fines<sup>5</sup> with particle sizes smaller than 100µm (Fuerstenau, et al., 2007).

### **Flotation Reagents**

Several types of reagents have been suggested for use in froth flotation of carbon fines, including collectors, frothers and depressants. Collectors, such as diesel or kerosene, are used to make carbon particles hydrophobic and facilitate their attachment to air bubbles. Frothers, such as methyl isobutyl carbinol (MIBC), are added to the slurry to stabilize the air bubbles and create a stable froth layer. Depressants, such as sodium silicate or sodium hexametaphosphate, are used to prevent unwanted minerals from attaching to the air bubbles and reduce the amount of waste generated (Chen, et al., 2019) (Zhang, et al., 2019).

---

<sup>5</sup> Figure 5. Sokolović, J.; Mišković, S. (2018). The effect of particle size on coal flotation kinetics: A review. *Journal. Physicochemical Problems of Mineral Processing*. 54. p. 1172-1190.

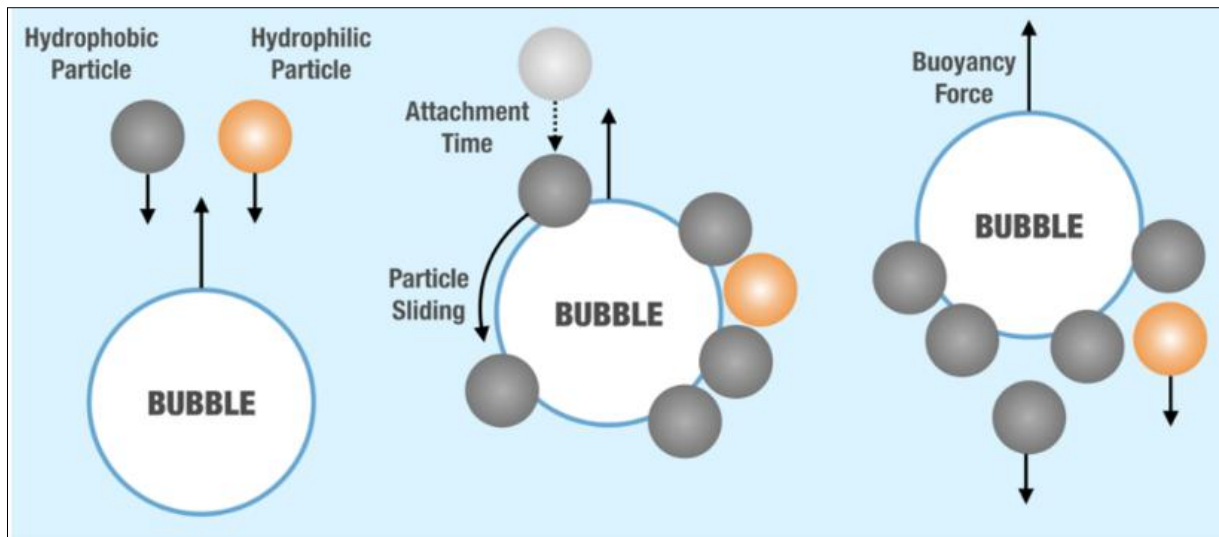


Figure 5: Mechanisms of particle-bubble interaction (Sokolović, J.; Mišković, S., 2018).

## Diesel

Diesel oil is sometimes used as a collector in froth flotation of carbon fines. The effectiveness of diesel as a collector is attributed to its ability to form a thin film on the surface of the carbon particles, which makes the particles more hydrophobic and thus more likely to attach to air bubbles and rise to surface of flotation cell. However, the use of diesel as a collector has some disadvantages. One of the main drawbacks is that diesel is a non-selective collector, meaning it can also attach to other minerals present in the ore, reducing the purity of the carbon concentrate. Additionally, diesel can pose environmental and health risks due to its toxicity and flammability (Gerson & Klemm, 1990).

## Kerosene

Kerosene is a hydrocarbon-based collector that is commonly used in froth flotation of carbon fines. It selectively wets the surfaces of carbon particles, allowing them to attach to air bubbles and rise to the surface for collection. The effectiveness of kerosene as a collector is influenced by various factors, such as particle size, pH and mineral impurities. Studies have shown that kerosene is particularly effective in flotation of high-ash carbon fines, but its use can also result in lower carbon recovery and increased ash content in the concentrate (Peng & Zhao, 2019) (Somasundaran & Harris, 1982).

## **Sodium Isopropyl Xanthate**

Sodium isopropyl xanthate (SIPX) is commonly used as a collector in froth flotation of carbon fines. SIPX imparts hydrophobicity to carbon particles which contain metal ions on their surface due to the presence of a thiol group. The formation of this complex xanthate on the carbon particle surface allows for them to bind with air bubbles and float to the froth layer in a flotation cell. The metal xanthate complex is stable and can withstand the mechanical and chemical stresses of the flotation process. The effectiveness of SIPX as a collector can be affected by various factors, such as the pH of the solution, the size and shape of the carbon particles and the presence of other minerals in the ore. It has been found that SIPX is most effective at a pH range of 6-10 and that it exhibits stronger collection efficiency with smaller and more irregularly shaped carbon particles (Gao & Liu, 2018).

## **Waste Bio-Oil**

The use of waste bio-oil as a frother in froth flotation of carbon fines is a relatively new area of research and there is limited information available on its chemistry. Bio-oils are usually obtained from biomass sources such as but not limited to wood or agricultural waste and are known to chemically contain phenols, ketones and aldehydes that are able to create a stable froth phase. Bio-oils are considered renewable and are a sustainable alternative to traditional frothers such as alcohols and glycols, which are derived from non-renewable sources. A recent study investigated the use of waste bio-oil as a frother in the flotation of graphite, a carbon mineral. The researchers found that waste bio-oil was effective in producing a stable froth and that the froth had a high liquid fraction, indicating good bubble-particle attachment. They suggested that the effectiveness of waste bio-oil as a frother may be due to its ability to interact with the water-air interface and create a stable film (Zhao, et al., 2021). However, the effectiveness of waste bio-oil as a frother may depend on various factors, such as the type and quality of the bio-oil, the pH of the solution and the size and shape of the carbon particles. Further research is needed to fully understand the potential of waste bio-oil as a frother in froth flotation of carbon fines (Gama, et al., 2020).

### **2.4.2.3 Carbon Ashing**

Carbon ashing is a process that involves heating the carbon fines in an oxygen-rich environment, which burns off the carbon and leaves behind a gold-rich ash. The process can be used to concentrate adsorbed gold and other inorganic material by removing the carbonaceous materials. Microwave augmented ashing is a variation of this process that uses microwave radiation to heat the carbon fines, resulting in faster and more efficient ashing. The process is effective for concentrating carbon fines up to particle sizes much smaller than 75µm (Gao, et al., 2018) which then follows direct cyanidation or smelting of the gold-rich ash. However, the process has potential environmental impacts, such as the emission of greenhouse gases and the generation of hazardous wastes (Gao, et al., 2018) (Lee, et al., 2012).

### **2.4.2.4 Ultrasonic Elution Method**

(Feng, et al., 2003) found that ultrasound can enhance the elution of gold from activated carbon, as studied in a lab-scale elution column and using ultrasonication<sup>6</sup> at 40kHz. This finding is consistent with (Hamdaoui, et al., 2005), who noted that the desorption of metals can occur in the presence of ultrasound and with (Breitbach, et al., 2003) who found that ultrasonic irradiation can improve the magnitude and rate of desorption. Additionally, (Yu, et al., 2003) observed that the addition of ethanol can also increase desorption rates. (Adam, 1994) conducted a study that showed that using sodium sulphide in its hydrous state, Na<sub>2</sub>S.9H<sub>2</sub>O, can achieve elution efficiencies of about 100% in as little as 4 hours at ambient temperatures of 25°C-30°C, making ultrasonic elution at room temperature and pressure a viable research objective.

---

<sup>6</sup> Figure 6. Industrial Quick Search. Ultrasonic Cleaning. Editorial. IQS Directory. <https://www.iqsdirectory.com/articles/ultrasonic-cleaners/ultrasonic-cleaning.html>. [Date Accessed: 25 May 2023]

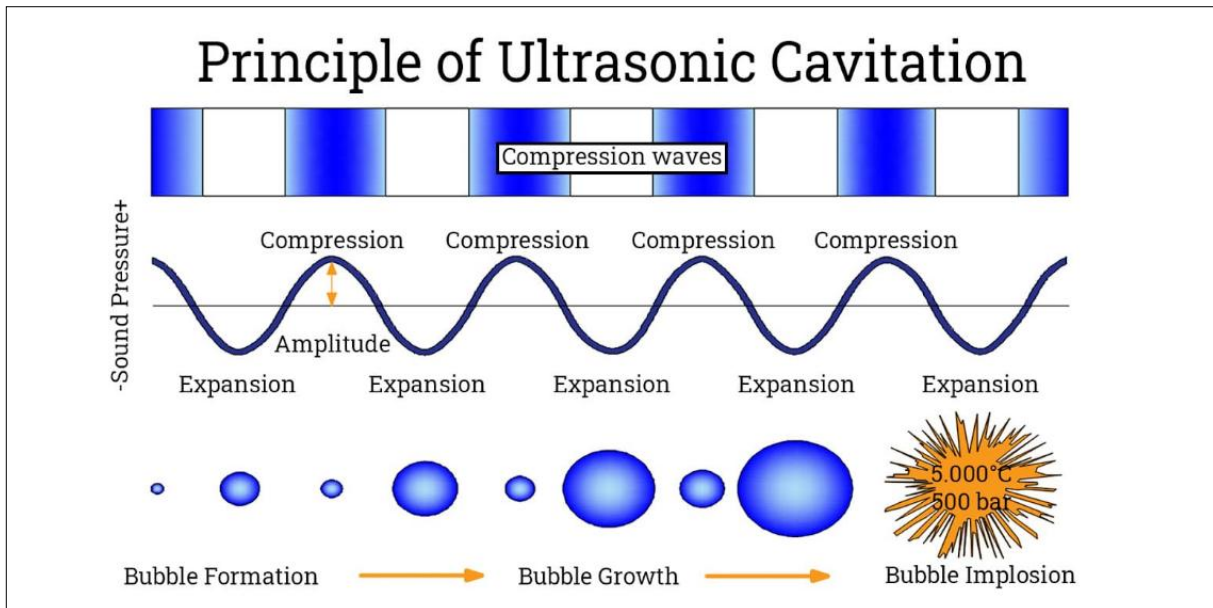


Figure 6: Principle of ultrasonic cavitation (Industrial Quick Search).

#### 2.4.2.5 Waste Material

Gold loaded carbon fines are a by-product of the gold mining process and are typically considered as waste material. Although the carbon fines contain a significant amount of gold, they are often discarded due to the difficulty and costs associated with recovering the gold. The disposal of gold loaded carbon fines can pose environmental and economic challenges. The fines can contain harmful pollutants e.g. cyanide and mercury, which seep into the environment and cause detrimental effects to human health and wildlife. Concurrently, gold lockup in unprocessed fines can translate into a notable and cumulative loss of revenue for mining companies, as the gold content is often enough significantly high. (Kolade, 2020).

#### 2.5 Economic Benefit from Processing Loaded Carbon Fines for Gold Recovery

The economic benefits of processing gold loaded carbon fines can be significant due to the high value of gold. The price of gold has maintained a somewhat stable trajectory and has been on the high in recent years, valued around US\$1,800 per Troy ounce in April 2023. Based on this price, a simple analysis of processing 1t of loaded carbon fines at a composite head grade of 500g/t would recover gold valued US\$9,000.00. The global gold mining industry generates several million tonnes of loaded activated carbon per year and a significant portion of this carbon is discarded

as waste material. It is estimated that the gold content of this waste carbon is in the range of several hundred thousand Troy ounces per year, providing potential revenue for gold mining companies (Adams, 2016).

## **2.6 Environmental Considerations in Processing Loaded Carbon Fines**

### **2.6.1 Froth Flotation**

Froth flotation is a commonly used method for concentrating carbon fines due to its high efficiency and selectivity. However, the process can have negative environmental impacts, including the generation of large amounts of waste and the release of pollutants. To mitigate these impacts, various strategies have been suggested, such as the use of alternative reagents that are less toxic and more environmentally friendly, the recycling of water and reagents and the use of closed-loop systems to reduce waste generation (Chen, et al., 2019) (Zhang, et al., 2019).

Alternative reagents are suggested to make froth flotation more environmentally friendly for concentrating carbon fines. For example, surfactants have been used as alternative collectors to diesel or kerosene, which are less toxic and more biodegradable (Chen, et al., 2019). Surfactants have lower toxicity and biodegradability compared to traditional collectors such as diesel or kerosene. The use of surfactants in froth flotation has been shown to improve the selectivity and efficiency of the process, leading to higher recovery rates and reduced waste generation (Chen, et al., 2019). Additionally, some surfactants have been shown to have a lower environmental impact than traditional collectors, with reduced greenhouse gas emissions and lower energy consumption during production (Kitchener, et al., 2019).

### **2.6.2 Ultrasonic Elution**

High-frequency sound waves used in ultrasonic elution can generate noise levels that may be harmful to human health and wildlife in the surrounding area. This means that employing ultrasound requires the installation of special soundproofing measures or other noise mitigation strategies to minimize associated negative impacts on the environment.

Ultrasonic elution can generate heat due to friction and vibration of the carbon fines, which can lead to increased energy consumption and greenhouse gas emissions. Additionally, the heat generated during ultrasonic elution may require additional cooling measures to prevent overheating and potential environmental damage (Zhang, et al., 2021).

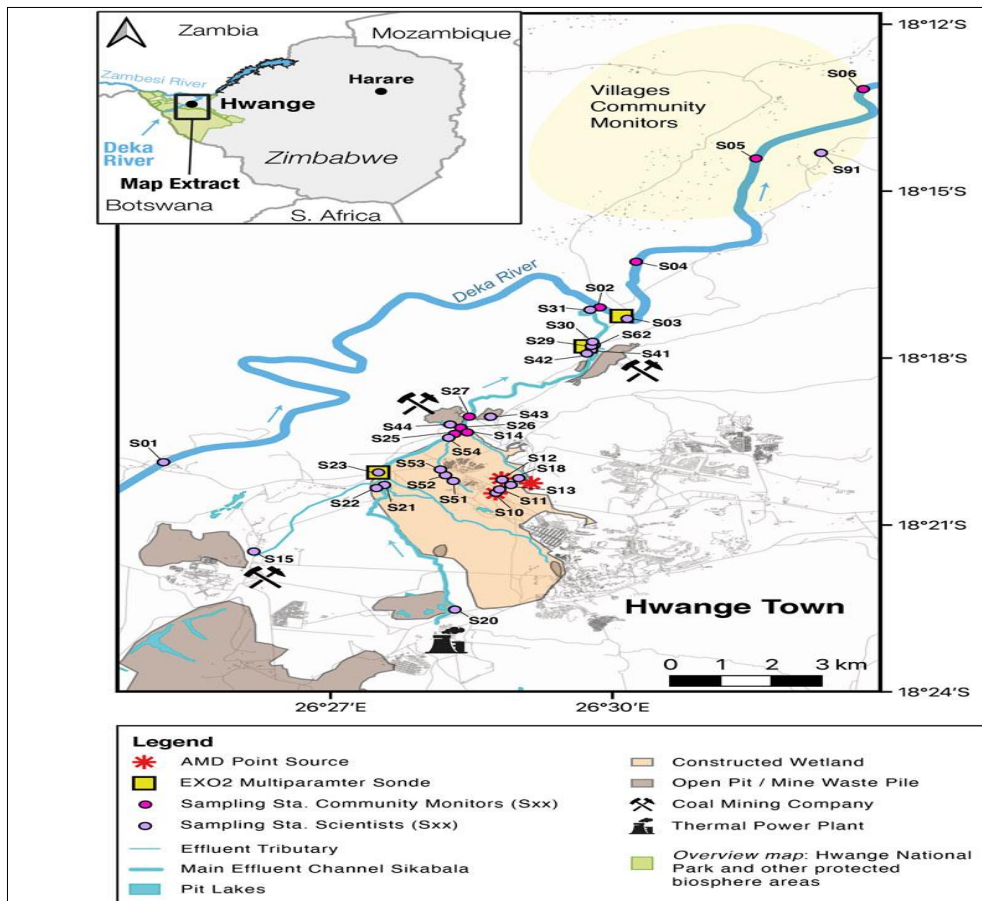


Figure 7: Overview map illustrating coal mining concessions and protected natural reserves in the Hwange District, Western Zimbabwe (2018).

## 2.7 Digitisation in Processing Loaded Carbon Fines

### 2.7.1 Froth Flotation

The use of machine learning and artificial intelligence algorithms can improve the accuracy and efficiency of mineral identification and optimise the selection of reagents and operating parameters (Gao, et al., 2020). Additionally, using advanced sensors and imaging technologies can provide real-time information on the froth surface, allowing for better control of the process and improved recovery rates

(Barbian, et al., 2019). The integration of these technologies can lead to reduced waste generation, improved energy efficiency and higher recovery rates. In a study by (Liu, et al., 2020), a machine learning algorithm was used to optimize the flotation process of coal fines. The algorithm was able to identify the most effective reagents and operating conditions to maximize the recovery of carbon and reduce the generation of waste.

At this stage, the lack of quality training data deems integrating machine learning algorithms immature to be applied at plant scale, as this could lead to inaccurate predictions and suboptimal operating conditions (Gao, et al., 2020). On top of that, the flotation process is fairly complex and the reliance on monitoring and optimising multi-layered variables poses a challenge in developing accurate and reliable machine learning models. (Li, et al., 2021) Incorporating machine learning requires modifications to the hardware and software used in the process, thereby incurring significant capital investment costs to the mining company (Barbian, et al., 2019).

The use of membrane filtration technologies such as ultrafiltration and nanofiltration, which remove impurities, opens up avenues in reusing process water and thereby reducing the reliance on potable water in flotation circuits. (Kawatra, et al., 2021) Similarly, advanced control systems and sensors aid in making the process environmentally and cost sustainable in the long-haul, by optimising water usage and reagents, reducing wastage and promoting energy efficiency. (Barbian, et al., 2019)

### **2.7.2 Ultrasonic Elution**

Digitalization and technological advancements have led to the development of more efficient and automated ultrasonic elution systems for carbon fines. Such systems use advanced sensors and controls for optimization and improved recoveries during elution. One such example is the use of real-time monitoring and control systems. This data is used to adjust parameters of ultrasonic elution in real-time, thereby making the system optimized for efficiency and negate any subsequent major environmental side effects.

Another way in which technology is being integrated in ultrasonic elution is through simulation and modeling software. These software tools can simulate the elution process and predict the behaviour of the carbon fines and eluting solution under different conditions. This allows for more accurate prediction of the efficiency of elution and the impact of different variables, such as particle size distribution and solution flow rate. (Zhang, et al., 2021)

## **2.8 Simulation**

### **2.8.1 Ultrasonic Elution Simulation using DWSIM**

DWSIM is open-source software tool and free to access. It is relatively easy to modify and customize based on the desired outcome. This makes it a good option for process engineers who may be working on limited budgets but would still require professional customization modeling features for simulation projects (Elias & Martínez, 2019). DWSIM offers advanced simulation capabilities, such as sensitivity analysis, optimization and uncertainty analysis. These features allow users to explore different scenarios and optimize the elution process for maximum efficiency and cost-effectiveness.

### **2.8.2 DWSIM & METSIM**

DWSIM and METSIM are two process simulation software tools that can be used to simulate ultrasonic elution of carbon fines. However, DWSIM has several advantages over METSIM. First, DWSIM has an intuitive user interface and drag-and-drop modeling capabilities, which make it easier for users to create process flow diagrams and define operating conditions without advanced programming knowledge. In contrast, METSIM has a steeper learning curve and may require more advanced programming skills to use effectively. Second, DWSIM includes an extensive library of pre-built models and components, which can be customized and combined to create comprehensive simulations of the elution process. Although METSIM also has a library of pre-built models, it may not be as extensive or customizable. Third, DWSIM is free and open-source, while METSIM requires a license fee, which could be a barrier for researchers or process engineers with limited budgets. Finally, DWSIM has been certified by AspenTech, which confirms its compatibility with AspenTech's simulation software and enhances its simulation capabilities. Overall,

DWSIM is a better choice than METSIM for simulating ultrasonic elution of carbon fines due to its user-friendly interface, open-source nature and Aspen certification. (Smith, 2023)

## **2.9 Mathematical Modeling**

The ultrasonic elution process can be represented through competent mathematical models, which take into account the multi-variable complexities to varying degrees of computing, such as temperature, pH and ultrasonic power, to mention a few. The models not only help in identifying and suggesting optimum operational conditions for gold elution using ultrasound, but also help to identify potential bottlenecks in the process and suggest strategies for improvement. Overall, the use of process modeling through mathematical models for monitoring ultrasonic elution of gold from loaded carbon can lead to significant benefits in terms of improved efficiency, higher yields and cost savings. (Murinda & al, 2018) (Chiririwa & al, 2016) (Jolly & al., 2014)

### **2.9.1 Benefits of using Mathematical Modeling**

In 2013, Zhang and Li developed a mathematical model to simulate the ultrasonic-assisted elution of gold from activated carbon. The model incorporated various parameters such as temperature, pH and ultrasonic power and was shown to accurately predict the elution efficiency. The authors note that the model can be used to optimize the elution process and reduce the consumption of reagents. (Zhang & Li, 2013 )

In 2020, Wang et al. developed a mathematical model to simulate the ultrasonic-assisted elution of gold from activated carbon. The model incorporated the effects of various factors such as in above mentioned study from 2013 and was shown to accurately predict the elution efficiency. The authors note that the model can be used to optimize the elution process and improve the efficiency and yield of gold recovery. (Wang & al., 2020)

### **2.9.2 Solving ODEs using Numerical Solutions**

Several studies in the literature have looked at the use of employing numerical methods to solve ODEs modeling the rate of loaded carbon elution. In 2019,

Manrique et al. used Euler's Method to solve the ODEs that model the dynamics of the gold elution process from activated carbon. The study found that this method provided them with reliable results, although it required a small time step size to achieve the desired accuracy. (Manrique & al., 2019 )

Similarly in 2015, Moyo et al. used the Runge-Kutta Method to solve ODEs, again to model the elution of gold from loaded carbon. Similarly, they found that this method also provided accurate results for their findings, although it was more computationally demanding than Euler's Method. Overall, both methods showed to provide accurate solutions in both instances, with the choice depending on the specific requirements of the problem at hand. (Moyo & al., 2015)

### 2.9.3 Other Types of Mathematical Models

#### 1. 2<sup>nd</sup> Order Reaction Model

This model assumes that the rate of elution is proportional to the square of the concentration of gold loaded onto the carbon, rather than linearly proportional as in the first-order model. The differential equation for this model is:

$$\frac{\delta(M_c * C_c)}{\delta t} = -k * M_c * C_c^2 \quad \text{Eq. 2}$$

#### 2. Elovich Model

This model assumes that the rate of elution decreases as the amount of gold loaded onto the carbon decreases, due to decreasing availability of active sites on the carbon surface. The differential equation for this model is:

$$\frac{\delta(M_c * C_c)}{\delta t} = -k * e^{-\beta C_c} \quad \text{Eq. 3}$$

where:

$\beta$  – constant connected to number of active sites on carbon surface

### 3. Avrami-Erofeev Model

This model assumes that the rate of elution is controlled by the nucleation and growth of gold particles on the carbon surface and that the rate of elution decreases as the number of active sites on the carbon surface decreases. The differential equation for this model is:

$$\frac{\delta(M_c * C_c)}{\delta t} = -k * (1 - e^{-at^n}) \quad \text{Eq. 4}$$

where:

$\alpha$  - constant connected to rate of nucleation of GLCF

$n$  - constant connected to number of active sites on carbon surface

## CHAPTER THREE: METHODOLOGY

### 3.0 PPE

Prior to carrying out experimental procedures, the researcher ensured the wearing of appropriate PPE, in adherence with 2022/23 SHE Regulations at CASE STUDY.

- Latex Gloves
- N95 Dust Mask
- PVC Gloves
- Safety Goggles
- Safety Hard Helmet
- Safety Shoes
- Worksuit

### 3.1 Sample Collection using Systematic Random Sampling

#### 3.1.1 Apparatus:

- 50kg sample bag
- PVC sheet plastic
- Riffle sample splitter
- 25 x 2kg sample bags
- Top-pan mass balance
- Stopwatch/timer
- Shovel

#### 3.1.2 Reagents & Materials

- Carbon-Grit mixture

#### 3.1.3 Procedure

1. Collect a 50kg sample of carbon-grit mixture from CIL 1 and CIL 2 stock yard and storage drums.  
Employ systematic sampling of stock yard piles by grabbing handfuls of carbon-grit mixture from different sections in order to have a fair sample representation.
2. Homogenize sample by thoroughly mixing for even carbon-grit ratios.
3. Split into 50 x 1kg samples and store in air tight sample bags.

### 3.2 Composite Head Assay using Fire Assay Method

Quantifying Au, Ag and Cu adsorbed onto activated carbon.

#### 3.2.1 Apparatus

- Bone ash cupels
- Cupellation furnace
- Test-tubes
- Test-tube tray
- Top-pan mass balance
- Stopwatch/timer
- Hot plate
- Beakers
- 200ml volumetric flasks
- Wash bottle
- Atomic Absorption Spectrophotometer (AAS)

#### 3.2.2 Reagents & Materials

- Hydrochloric acid (HCl)
- Nitric acid (HNO<sub>3</sub>)
- Aqua regia
- Borax
- Flux
- Silver wire
- Carbon sample
- Distilled water

#### 3.2.3 Procedure

1. Weigh 0.5g of the carbon sample and place in a cupel.
2. Roll 1cm of silver wire and add to the bone ash cupel.
3. Add 2g of borax and 5g of flux to the cupel and insert the cupels into a cupellation furnace at 950 °C for one hour.
4. After one hour, remove cupels from the furnace and allow to cool to room temperature.
5. Hand-pick resulting gold prills and add to beakers for dissolution.
6. Add Aqua regia to each beaker and place on a hot plate at 250 °C for 10 minutes. Aqua regia is 1 part HNO<sub>3</sub>: 3 parts HCl.
7. After silver is fully digested, remaining bead is water washed twice using distilled water.

8. Add 10ml of HCL to the remaining prill in the beaker and place the beakers onto the hot plate until all the gold is dissolved.
9. When prill is completely digested, the contents of the beaker are transferred to 200ml volumetric flasks.
10. Add hot distilled water into the 200ml volumetric flasks up to the mark and mix thoroughly to ensure homogeneity.  
This dilutes the samples to a concentration that allows for reading.
11. Read solution samples for Au, Ag and Cu on the Atomic Absorption Spectrophotometer.  
Record appropriately.

### **3.3 Particle Size Distribution (PSD) of Raw Carbon-Grit**

PSD was conducted as part of characterizing raw carbon-grit sample.

#### **3.3.1. Apparatus**

- Sieves (4.75mm, 3.35mm, 2.80mm, 2.00mm, 1.70mm, 1.18mm, 850 $\mu$ m and - 850 $\mu$ m sieves)
- Mechanical sieve shaker
- Top-pan mass balance
- Stopwatch/timer

#### **3.3.2. Reagents & Materials**

- Carbon-grit sample

#### **3.3.3. Procedure**

1. Arrange sieves in order of decreasing size of aperture onto sieve shaker.
2. Weigh 1,600g of carbon-grit sample and pour into first sieve.  
Cover and seal using lid for sieve shaker.
3. Switch on sieve shaker and run for 10 minutes.  
Agitation is used to aid the movement of carbon within and between the sieves.
4. Amount of material retained in each sieve is measured and recorded.
5. 2  $\times$  5g samples of the middlings retained at each size fraction are obtained, appropriately labeled and submitted for carbon analysis for Au, Cu and Ag assay.

### 3.4 Abrasion Test of Carbon-Grit

Abrasion Test was conducted as part of characterizing carbon-grit sample.

#### 3.4.1. Apparatus

- Oven
- Sieves (1.70mm, 2.00mm and 850 $\mu$ m sieves)
- Plates
- Top-pan mass balance
- Stopwatch/timer
- 4L standard flotation cell
- Denver flotation machine

#### 3.4.2. Reagents & Materials

- Carbon-grit sample
- Tap water

#### 3.4.3. Procedure

1. Wash approximately 500g of carbon-grit sample using tap water.
2. Transfer to a plate and dry in an oven at 110°C for at least 8 hours.
3. Allow the carbon to cool and screen the carbon using sieve sizes 1.70mm and 2.00mm.
4. Weigh 30g of carbon-grit mixture in duplicate.  
You should have 2 samples of 30g each.

##### (a) Conditioning Abrasion

1. Measure and pour 3L of tap water into the 4L standard flotation cell of the Denver flotation machine, turn on and open air nozzle.  
Flotation cell must be preset to 1200r.p.m.
2. Add 30g of activated carbon to the cell of the Denver flotation machine and allow cell to run for 20 minutes.
3. Stop the cell and screen the activated carbon through an 850 $\mu$ m screen.
4. Transfer the carbon remaining on the screen to plate and dry it at 110  $\pm$  10°C for at least 8 hours.
5. When dry, manually screen the activated carbon through the 850 $\mu$ m screen for about 5 minutes.  
Discard fines that collect on the pan.
6. Place a clean, plate on a top-pan balance and tare.

7. Quantitatively transfer the carbon retained by the screen and weigh.

$$\text{Conditioning weight} = \text{weight of carbon retained by screen} \quad \text{Eq. 5}$$

### **(b) True Abrasion**

1. Repeat as for “Conditioning Abrasion” steps, except that the duration of mixing must be exactly 2 hours.

$$\text{True weight} = \text{weight of carbon retained by screen} \quad \text{Eq. 6}$$

## **3.5 Preparation of Sample A**

This was achieved through a Particle Size Distribution of the carbon-grit mixture.

### **3.5.1 Apparatus**

- Sieves (2.00mm, 1.70mm and 1.18mm sieves)
- Mechanical sieve shaker
- Top-pan mass balance
- Stopwatch/timer

### **3.5.2 Reagents & Materials**

- 11kg carbon-grit sample

### **3.5.3 Procedure**

1. Arrange sieves in order of decreasing size of aperture onto sieve shaker.
2. Weigh 1600g of carbon-grit sample and pour into first sieve.  
Cover and seal using lid for sieve shaker.
3. Switch on sieve shaker and run for 10 minutes.  
Agitation is used to aid the movement of carbon within and between the sieves.
4. Amount of material retained in each sieve is measured, recorded, labeled and stored in respective sample bags.  
Total mass of middlings in the three size fractions should approximate 700g.  
Therefore, each sieve middling mass falls between the range 172g - 396g of carbon grit.

5. Repeat steps 1 through 4, seven more times or until you have 36 x 100g sample bags of carbon-grit middlings sized 2.00mm, 36 x 100g of carbon-grit middlings sized 1.70 mm and 36 x 100g of carbon-grit middlings sized 1.18 mm.

This makes a total of 108 sample bags of carbon-grit weighing at least 100g each.

These three size fractions shall be classified under “Sample A”.

6. 2 × 5g samples each of Sample A as a composite of the three size fractions are obtained, appropriately labeled and submitted for carbon analysis for Au, Cu and Ag assay.

### **3.6 Preparation of Sample B**

#### **3.6.1 Milling Carbon-Grit Mixture**

The carbon-grit sample was homogenized in size through implementing a grinding stage.

##### **3.6.1.1 Apparatus**

- Lab scale rod mill
- Standard stainless steel rods
- 5 x 1kg dishes
- Top-pan mass balance
- Stopwatch/timer
- Sieve (1.18mm sieve)
- Mechanical sieve shaker

##### **3.6.1.2 Reagents & Materials**

- 11kg carbon-grit sample

##### **3.6.1.3 Procedure**

1. Fill rod mill between 45-48% with rod mills.
2. Weigh 1kg of carbon-mixture and pour into rod mill.  
Safely secure mill onto rollers and lock catch screen.
3. Run rod mill for 10-13 minutes.
4. Empty powder carbon-grit mixture into dish.
5. Using a mechanical sieve shaker, dry sieve the powdered carbon-grit mixture through a 1.18mm screen for 10 minutes.

Re-grind oversize that collect onto of screen.

6. Obtain 11kg of sample for the next stage.

### **3.6.2 Preparation of Sample B**

This was achieved through a Particle Size Distribution of the ground carbon-grit mixture.

#### **3.6.2.1 Apparatus**

- Sieves (850 $\mu$ m, 75 $\mu$ m, 53 $\mu$ m sieves)
- Mechanical sieve shaker
- Top-pan mass balance
- Stopwatch/timer

#### **3.6.2.2 Reagents & Materials**

- 11kg ground carbon-grit sample

#### **3.6.2.3 Procedure**

1. Arrange sieves in order of decreasing size of aperture onto sieve shaker.
2. Weigh 1600g of the ground carbon-grit sample and pour into first sieve. Cover and seal using lid for sieve shaker.
3. Switch on sieve shaker and run for 60 minutes.  
Agitation is used to aid the movement of carbon within and between the sieves.
4. Amount of material retained in each sieve is measured, recorded, labeled and stored in respective sample bags.  
Total mass of middlings in the three size fractions should be no greater than 1600g.  
Therefore, each sieve middling mass falls between the range 300g - 800g of carbon grit.
5. Repeat steps 1 through 4, three more times or until you have 36 x 100g sample bags of carbon-grit middlings sized 850 $\mu$ m, 36 x 100g of carbon-grit middlings sized 75 $\mu$ m and 36 x 100g of carbon-grit middlings sized 53 $\mu$ m.  
This makes a total of 108 sample bags of carbon-grit weighing at least 100g each.  
These three size fractions shall be classified under "Sample B".

6.  $2 \times 5\text{g}$  samples each of Sample B as a composite of the three size fractions are obtained, appropriately labeled and submitted for carbon analysis for Au, Cu and Ag assay.

### **3.7 Specific Gravity (SG) Test of Sample A & Sample B**

SG Test was conducted as part of characterizing Sample A and Sample B.

#### **3.7.1 Apparatus**

- Top-pan mass balance
- 500ml beaker

#### **3.7.2 Reagents & Materials**

- 500g Sample A composite
- 500g Sample B composite

#### **3.7.3 Procedure**

1. Place empty 500ml beaker onto mass balance and tare.
2. Fill beaker to 70g of Sample A.  
Level and shake until no air spaces are left within sample.  
Record mass obtained.
3. Note volume occupied by mass obtained by reading value measured from the beaker.  
Record masses and their corresponding volumes respectively
4. Repeat steps 1 – 3 for 100g, 250g with Sample A composite.
5. Perform steps 1 – 4 with Sample B composite.

$$\text{SG} = \text{mass of carbon-grit mixture} / \text{volume of carbon-grit mixture} \quad \text{Eq. 7}$$

### **3.8 Concentrating Carbon through direct Froth Flotation**

Sample A size fractions and Sample B size fractions each, respectively, underwent froth flotation tests varying collector-frother ratios, as means to observe and compare the effect, if any, that these two variables have on efficiency of carbon concentrate recovery.

### 3.8.1. Apparatus

- Denver flotation machine
- 2L and 3L flotation cells
- Scrappers
- Metal plates
- Top-pan mass balance
- Stopwatch/time

### 3.8.2 Reagents & Materials

- 8kg Sample A (size fractions 2.00mm, 1.70 mm and 1.18 mm)
- 8kg Sample B (size fractions 850 $\mu$ m, 75 $\mu$ m and 53 $\mu$ m)
- Distilled water
- Hydrated Copper (II) sulphate (CuSO<sub>4</sub>) (Activator)
- 2L Sodium iso-propyl xanthate (SIPX) (Collector)
- 1L Betamin DZT545 (DZT545) (Depressant)
- 2L Diesel (Collector)
- 2L Kerosene (Collector)
- 2L Waste bio-oil (Frother)

### 3.8.3 Procedure

#### (a) Sample A (size fractions 2.00mm, 1.70mm and 1.18mm):

1. Mix 2L of distilled water with 100g of Sample A size fraction 2.00mm in a 2L Denver flotation cell.
2. Set agitator to 1200r.p.m and switch on the Denver flotation cell. Leave to run for 4 minutes.
3. After 4 minutes, turn on air flow to 3.0L/min.
4. Add 20cm<sup>3</sup> of 5% CuSO<sub>4</sub>(aq) and 24ml of collector-frother combination, where collector-frother combination =

[ (1) K + S , (2) D + S , (3) K + D + S , (4) K + WBO , (5) D + WBO , (6) K + D + WBO , (7) S + WBO , (8) S + WBO + K , (9) S + WBO + D , (10) S + WBO + K + D ]

Table 1: Volumes added per single run through of flotation test procedure

Test	S	V/ml	Test	WBO	V/ml	Test	S	&	V/ml
1	K + S	12 ; 12	4	K	+ 12 ; 12	7	S	+	12 ; 12
				WBO			WBO		
2	D + S	12 ; 12	5	D	+ 12 ; 12	8	S	+	8 ; 8 ; 8
				WBO			WBO	+	
							K		
3	K + D + S	8 ; 8 ; 8	6	K + D + WBO	8 ; 8 ; 8	9	S	+	8 ; 8 ; 8
							WBO	+	
							D		
						10	S	+	6 ; 6 ; 6
							WBO	+	; 6
							K + D		

Leave to run for 4 minutes.

5. Add 4 drops of DZT545 to the flotation cell.
6. On froth production, scrape off froth and concentrate every 15 seconds or as necessary.

Run flotation cell for 30 minutes.

This makes up the Rougher-Cleaner stage of froth flotation.

7. After 30 minutes, the froth concentrate and tail were collected, washed and placed in an oven to dry at 50°C.
8. To calculate the mass pull (%) at Rougher-Cleaner stage, Mass Pull<sub>RC</sub>, dry mass of froth concentrate and dry mass of tail (tail obtained before Rougher-Scavenger stage) was obtained and used via the following equation:

$$\text{Mass Pull}_{RC} (\%) = \left[ \frac{\text{Dry Mass of Concentrate}}{\text{Dry Mass of Feed Material (100g)}} \right] * 100 \quad \text{Eq. 8}$$

9. Repeat steps 1 – 6 (using same collector-frother combination), instead using the initial feed as the tail obtained from previous flotation (dried tail from) step 7.

Run flotation cell for 15 minutes.

This makes up the Rougher-Scavenger stage of froth flotation.

10. After 15 minutes, the froth concentrate and tail were collected, washed and placed in an oven to dry at 50°C.
11. To calculate the mass pull (%) at Rougher-Scavenger stage, Mass Pull<sub>RS</sub>, dry mass of froth concentrate was obtained and used via the following equation:

$$\text{Mass Pull}_{\text{RS}} (\%) = [\text{Dry Mass of Concentrate} / \text{Dry Tail Mass from step 7}] * 100 \quad \text{Eq. 9}$$

12. Record mass pull obtained in a table of Size Fraction against Collector Combination.
13. Repeat steps 1 – 12, with Sample A size fraction 1.70 mm then 1.18 mm, respectively.

**(b) Sample B (size fractions 850µm, 75µm and 53µm):**

Repeat froth flotation steps as highlighted in the above procedure but instead, use Sample B size fractions.

### 3.9 Ultrasonic Elution of Carbon Froth Concentrate

DWSIM was used to create a simulation of an elution column with an ultrasound setup as shown on the schematic on Figure 8 below.

#### 3.9.1 Apparatus

- 2.0cm x 7.0cm elution column
- Peristaltic pump
- Eluant tank
- Variable ultrasonic bath
- Water bath
- Shell-in-tube heat exchanger

#### 3.9.2 Reagents & Materials

- Potable/de-ionised water
- Carbon concentrate composite
- Sodium Hydroxide (NaOH)

### 3.9.3 Simulation Procedure

#### 1. Simulation Model

- Discrete event simulation in DWSIM software.
- Raoult's Law package for input and output objectives.

#### 2. Simulation Objectives

- To achieve steady-state at temperature less than 128°C and pressure less than 300kPa.

#### 3. Input Parameters

1. [478g/t Loaded Carbon] - Temperature = 25°C,  $f = 40\text{kHz}$ , Pressure = 101kPa,  
Mass Flow = 1,000kg/h, Molar Flow = 6.48kmol/h

2. [128W Ultrasound Power]

3. [2.5% w/v NaOH Eluant] - Temperature = 25C, Pressure = 101kPa,  
Mass Flow = 5.65kg/h, Molar Flow = 0.14kmol/h

4. [Circulating Water] - Temperature = 25C, Pressure = 101kPa,  
Mass Flow = 20kg/h, Molar Flow = 1.11kmol/h

5. [40kHz Ultrasonic Frequency]

6. [Peristatal Pump] - Vertical Head = 72.88m, Head = 899kPa, Efficiency = 75,  
Temperature Diff = 0.13C, Outlet Pressure = 1,000kPa

#### 4. Simulation Process Flowsheet

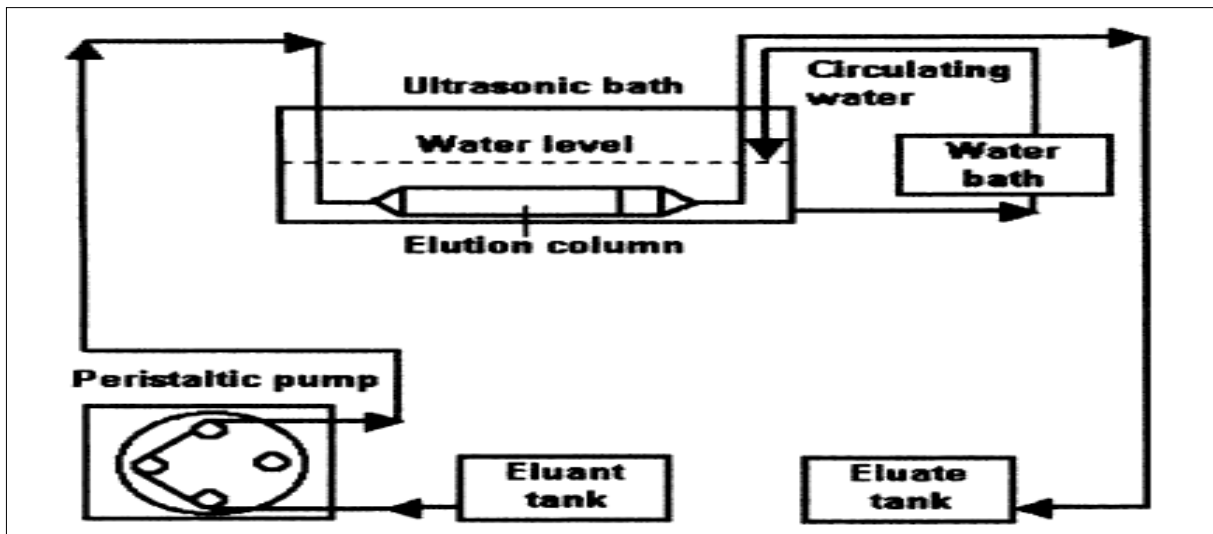


Figure 8: Ultrasonic elution schematic (Feng, D. et all, 2002).

#### 5. Output Metrics

1. [478g/t Eluate] - Temperature = 84 °C, frequency = 40kHz, Pressure = 101kPa,  
Mass Flow = 44kg/h, Molar Flow = 3.32kmol/h

2. [0g/t Stripped Carbon] - Temperature = 84 °C, frequency = 40kHz, Pressure =  
101kPa, Mass Flow = 44kg/h, Molar Flow = 0kmol/h

3. [Water In-Water Out] - Temperature = 85 °C, Pressure = 101kPa,  
Mass Flow = 5980.12kg/h, Molar Flow = 331.94kmol/h

#### 6. Experimental Design

- Parameters set to fixed pre-determined values.

#### 7. Assumptions & Limitations

##### Assumptions

1. Elution is a first-order reaction with respect to  $C_{(s)}[Au]$

$$\therefore \frac{\delta E}{\delta t} \propto C_{(s)}[Au] \quad \text{Eq. 10}$$

2. No Mass Transfer resistance

$$\therefore e_{(aq)}[Au] \leftrightarrow C_{(s)}[Au] \quad \text{Eq. 11}$$

3. Elution is homogenous chemical reaction.

4. Ultrasonic wave energy enhancing elution kinetics.

5. System is under steady-state conditions.

6. Model does not account for external factors affecting elution e.g. changes in pH, flowrate, etc.

7. Model may not be applicable to all systems and requires further validation through experimental data analysis.

## Limitations

- Elution process is dynamic, heterogenous and experiences Mass Transfer resistance due to thermodynamics of the gold dissolution process.

## 8. Validation & Verification

- Aspen certified simulation model.
- Recommend the following lab scale experimental tests -

### 1. Mass Transfer Experiments

Perform experiments using loaded carbon of varying gold loadings. Then measure the efficiency of elution under each condition. This aids in determining the direct effect of mass transfer resistance on elution efficiency. Compare obtained experimental values with the model assumption of an equilibrium that exists between gold concentration in the carbon and gold concentration in the eluant.

## **2. Elution Kinetics Experiments**

Perform elution experiments using loaded carbon under the same conditions as used in the model and measure gold concentration in the eluant at different time intervals. This enables the experimental determination of rate constant,  $k$ , for elution and it can be comparable with the model prediction.

## **3. Ultrasonic Wave Energy Experiments**

Perform elution experiments using ultrasonic baths with variable power and frequency. Then measure efficiency of elution under each of those conditions. This step allows the determination of a relationship that exists, if any, between the ultrasonic wave energy input and rate of elution. Value obtained can be compared against one predicted by the model.

## CHAPTER FOUR: RESULTS & DISCUSSION

### 4.0 Introduction

In this chapter, raw data was summarised, examined and interpreted to highlight the key findings obtained from experimental procedures covered in Chapter 3. This was achieved mainly through the use of graphs, other visual aids and mathematical modeling. The trends observed were then linked to relevant theory, therefore showing how monitored variables affected efficiency of froth flotation and ultrasonic-based elution. The following known assumptions were used as basis for all calculations:

- 1ppm = 1g/t
- 1% = 10,000ppm
- 1ml = 1g (distilled water)
- 1 Troy ounce<sup>7</sup> = 31.103g
- Activated Carbon SG = 0.50
- Gold price used at stated dates

### 4.1 Characterisation Results

#### 4.1.1 Particle Size Distribution & Gold Deportment Analysis

Particle Size Distribution (PSD) analysis was performed in order to select the most appropriate processing method for the carbon-grit sample. As shown in Appendix A-4, PSD analysis determines the size distribution of particles in a sample and the gold deportment analysis then informs on the distribution of gold in the sample.

---

<sup>7</sup> The standard weight measurement for Precious Metals is the Troy ounce. 1oz = 31.103g

#### 4.1.1.1 Raw Carbon Grit Sample Analysis

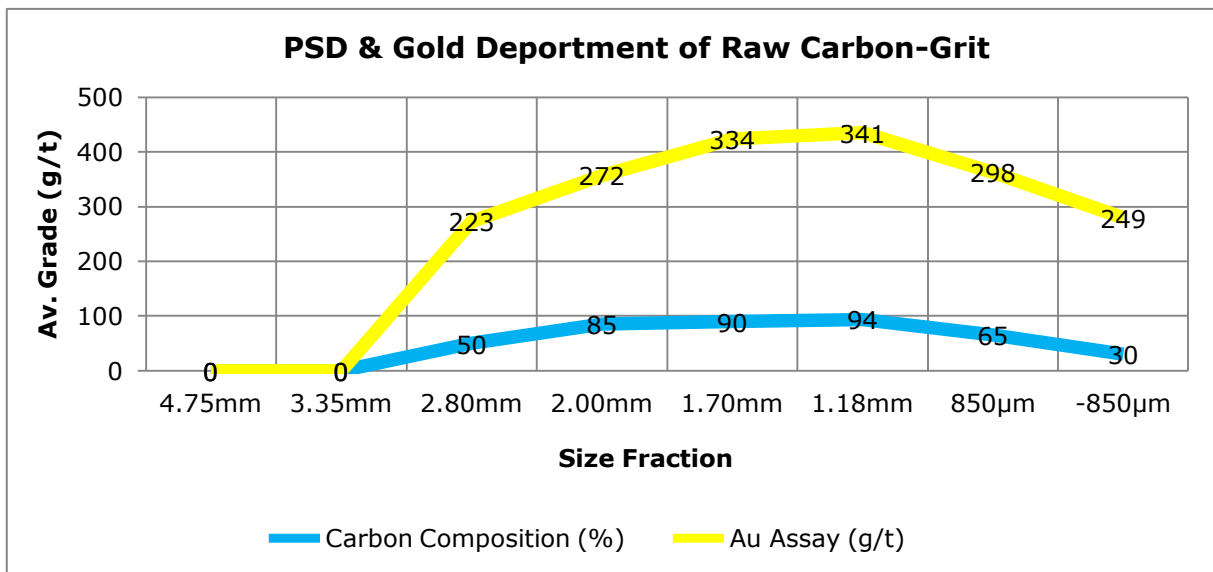


Figure 9: PSD and gold department of raw carbon-grit sample.

The largest size fraction, +4.75mm, was found to contain mostly chaff, grass, wood and/or rubber. Carbon was first noted at -3.35mm+2.80mm, making up 50% of the total carbon-grit sample at that size fraction. Trend line shows that gold department gradually increased, along with carbon composition, as the particle size also gradually decreased, peaking at -1.70mm+1.18mm, to then gradually decrease afterwards. (similar to graph of  $y = -x^2$ )<sup>8</sup>.

It was observed that the highest carbon composition of between 85-94% of the total carbon-grit sample was found at size fractions corresponding to -2.80mm+2.00mm, -2.00mm+1.70mm and -1.70mm+1.18mm, respectively. These three size fractions also contained the highest Au assay at an average composite head grade of 316g/t.

Under further investigation of the raw carbon-grit sample, a carbon composition of 30% of the total carbon-grit sample was found to contain much finer carbon of size fraction -850µm. Literature suggests that on average, the smaller the carbon size fractions, the larger the expected Au assays. This is due to the increase in residence time of the attritioned and chipped carbon particles which escape the counter-current flow through the screens due to their size, thereby adsorbing more gold in the

<sup>8</sup> The graph of  $y=-x^2$  shows a non-linear relationship between two variables, with a downward opening parabola representing a decrease in one variable squared with an increase in the other variable and is commonly used to display data in various fields.

CIP/CIL circuit. This is in comparison to courser carbon size fractions/particles, which would experience the normal residence time of approximately 28-35 hours.

However, no conclusive deduction on the extent to which this effect applies can be made from the experimental trend obtained due to the unavailability of a larger experimental data set that would have perhaps provided more extensive findings to conclude the extent to which this phenomena can be attributed.

#### 4.1.1.2 Sample A & Sample B Analysis



Figure 10: Sample A size fraction, 2.00mm.



Figure 11: Sample A size fraction, 1.70mm.



Figure 12: Sample A size fraction, 1.18mm.

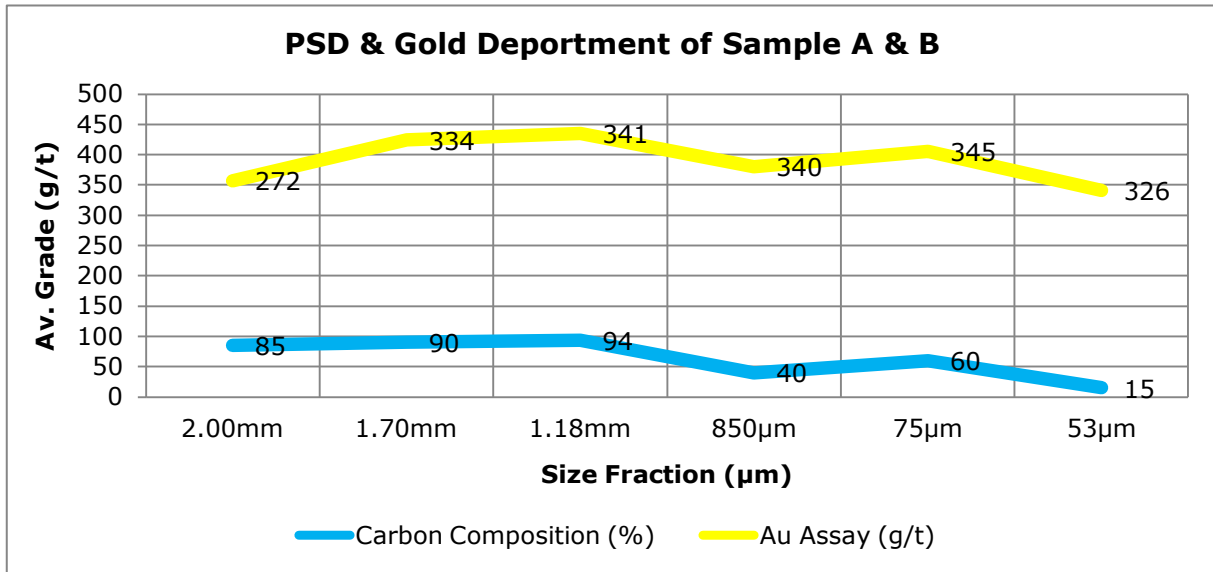


Figure 13: PSD and gold department of Sample A and Sample B.

PSD analysis on Sample A and Sample B obtained three distinct “larger” particle size fractions for A and three distinct “smaller” particle size fractions for B, as shown by the following empirical representation:

$$\text{Sample A} = [-2.80\text{mm}+2.00\text{mm}; -2.00\text{mm}+1.70\text{mm}; -1.70\text{mm}+1.18\text{mm}]$$

$$\text{Sample B} = [-1.18\text{mm}+850\mu\text{m}; +850\mu\text{m}-75\mu\text{m}; -850\mu\text{m}+53\mu\text{m}].^9$$

The average head grades for the aggregates of Sample A and Sample B are each shown below:

<sup>9</sup> Special Note: “Sample A” and “Sample B” are basket terminologies that only emphasise the size of the individual particles that fall under two corresponding categories. “Sample A” refers to coarser, larger size fractions and “Sample B” refers to finer, smaller size fractions. Otherwise, each size fraction is to be understood as its own standalone sample to be investigated in the subsequent analyses.

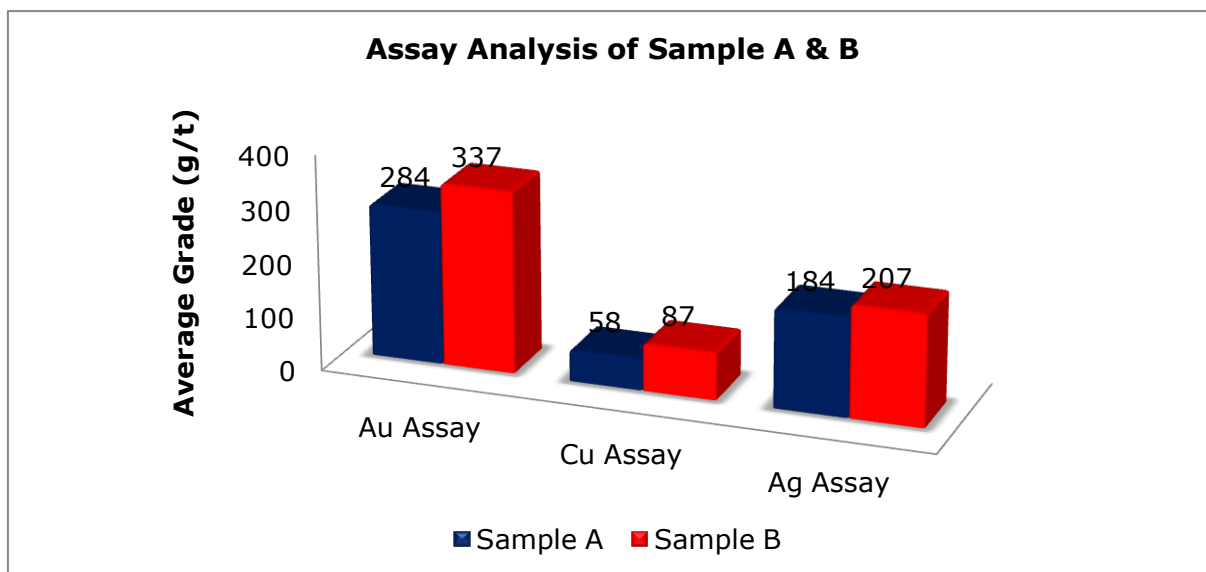


Figure 14: Assay analysis of Sample A and Sample B.

As supported by previously stated literature, the smaller size fractions of Sample B contained carbon of a higher average Au head grade of 337g/t and the somewhat courser size fractions of Sample A contained carbon at a lower average Au head grade of 284g/t.

The presence of copper and silver in the loaded carbon indicates that gold was adsorbed along with small percentages of base metals present in the leached solution, at an average of 73g/t and 196g/t over both samples respectively. The presence of iron (not covered by the scope of this research) is worth mentioning due to the chemical nature of gold ore mined at CASE STUDY.

#### 4.1.2 Effect of Physical Properties of Sample A & Sample B

##### 4.1.2.1 Specific Gravity<sup>10</sup> Analysis

A Specific Gravity (SG) test was performed on Sample A and Sample B in order to come up with optimum froth flotation conditions, specifically in terms of w/v of water to be added to the flotation cell. As a control measure, a Specific Gravity test was performed on virgin Donau 6x12 activated carbon, in order to extrapolate known

<sup>10</sup> Specific Gravity or relative density is a ratio, which measures the density of a substance in comparison to the density of water. This value simply shows whether a substance will float or sink, as  $SG > 1$  means sink and  $SG < 1$  means float in water at its most dense state at 4°C.

chemical surface properties of carbon onto the carbon-grit samples and suggest suitable reagents.

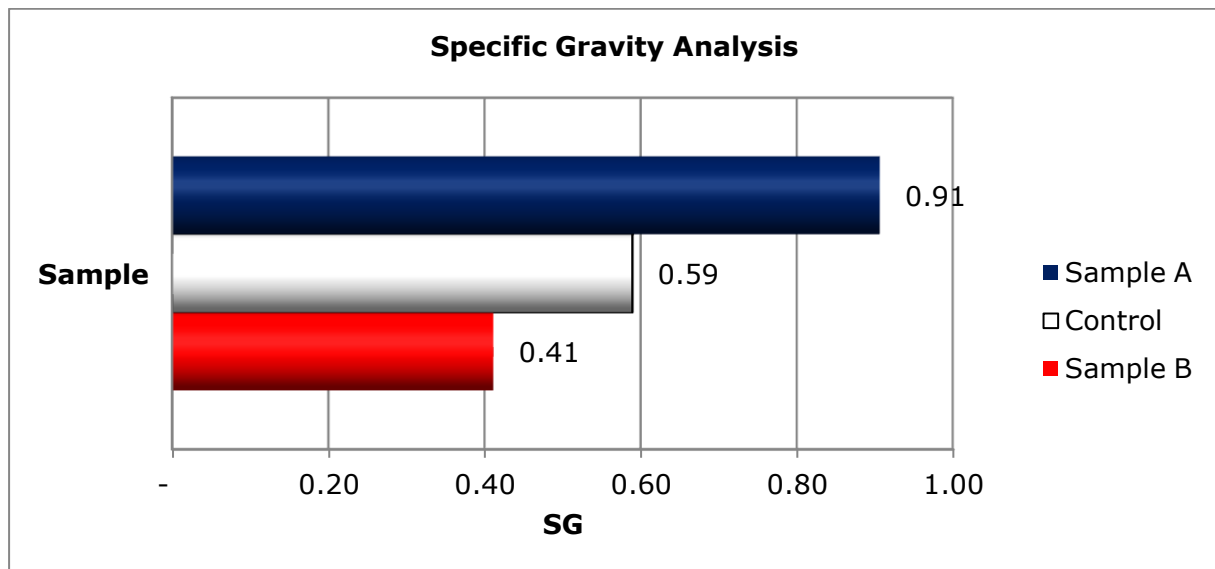


Figure 15: SG analysis of Sample A and Sample B.

From the figure above, Sample A has an implied lower flotability with an SG of 0.91 whereas Sample B has a higher implied flotability, only comparable at the same BV as Sample A, with SG 0.41. These figures can be compared with the control having an SG of 0.59, pitted against the industry standard activated carbon SG of 0.5.

#### 4.1.2.2 Abrasion Test<sup>11</sup> Analysis

An Abrasion test was performed on Sample A and Sample B in order to evaluate the wear resistance of the loaded carbon size fractions. This test helped to observe and ensure that the carbon would not break down during the froth flotation process, which could have resulted in the loss of gold particles into solution. As a control measure, an Abrasion test was performed on virgin Donau 6x12 activated carbon, in order to compare average abrasion rate of the two CIL/CIP carbon samples against a virgin carbon sample.

<sup>11</sup> An Abrasion test measures the resistance of a material to wear and tear. It is used to evaluate the durability and longevity of activated carbon samples for various industrial and consumer applications, e.g. in CIP/CIL applications.

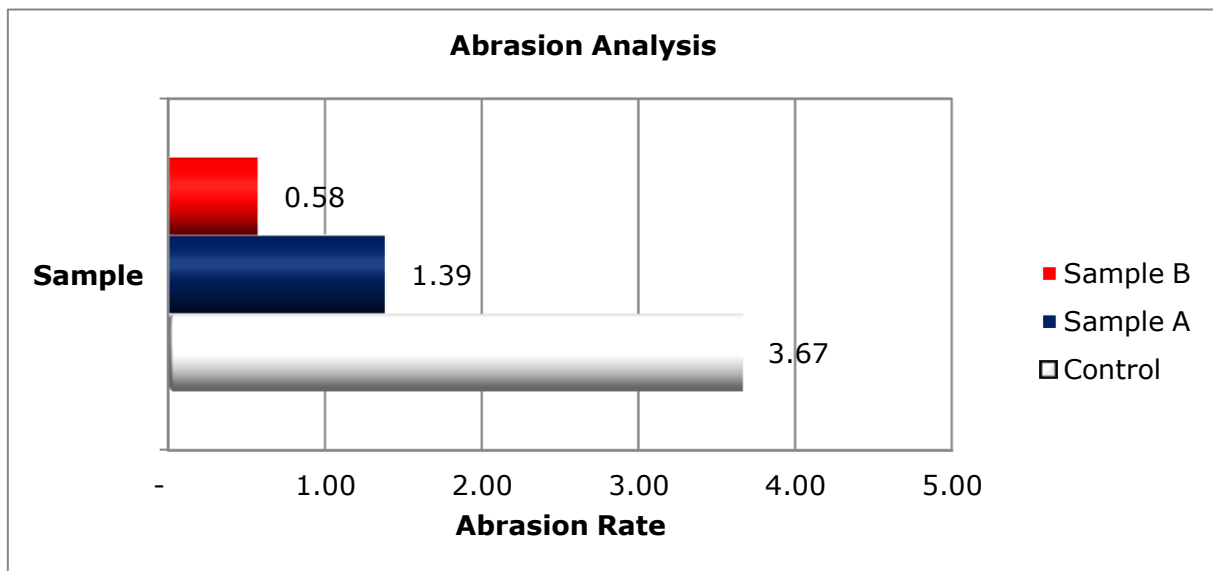


Figure 16: Abrasion analysis of Sample A and Sample B.

Sample A and Sample B both showed lower abrasion rates due to the nature of the carbon particles which are the result of the parent coarse carbon having undergone wear and attrition in the CIP/CIL circuit, as compared to abrasion rate obtained from virgin carbon of 3.67%. It can be concluded that gold losses due to the breaking down of Sample A and Sample B carbon particles during froth flotation can be considered negligible and will not have a significant effect on expected gold recovery in the subsequent ultrasonic elution.

#### 4.2 Froth flotation for Carbon-Grit Separation<sup>12</sup>

Three size fractions from Sample A and three size fractions from Sample B (making a total of six size fractions) were individually floated against each of the ten collector-frother combinations, respectively, as shown in Appendix B. It is worth mentioning that according to the literature and as a control measure, Diesel (D), Kerosene (K) and SIPX were strictly considered as collectors and Waste Bio-Oil (WBO) was considered as the only frother.

<sup>12</sup> Froth flotation for carbon-grit separation is a process that involves selectively separating hydrophobic carbon particles from hydrophilic grit by using air bubbles to attach to and lift the carbon particles into the froth concentrate phase, while the hydrophilic materials remain suspended in the bulk solution.

Table 2: C-F Combination Identities

Combination Identity	Key
K + S	Kerosene + SIPX
D + S	Diesel + SIPX
K + D + S	Kerosene + Diesel + SIPX
K + WBO	Kerosene + Waste Bio Oil
D + WBO	Diesel + Waste Bio Oil
K + D + WBO	Kerosene + Diesel + Waste Bio Oil
S + WBO	SIPX + Waste Bio Oil
S + WBO + K	SIPX + Waste Bio Oil + Kerosene
S + WBO + D	SIPX + Waste Bio Oil + Diesel
S + WBO + K + D	SIPX + Waste Bio Oil + Kerosene + Diesel

#### 4.2.1 Effect of Size Fraction on Mass Pull

To measure the effectiveness of froth flotation in separating carbon from grit, flotation yields were calculated based on the principle of Mass Pull<sup>13</sup> per size fraction, as indicated by Appendix B-1 and Appendix B-2. The relationship between froth flotation efficiency and size of particles is illustrated below:

<sup>13</sup> Mass Pull is a measure of how much of the feed sample reports to the froth concentrate only as carbon while grit remains suspended in the tail, i.e.

Mass Pull (%) = [Dry Mass of Froth Concentrate / Dry Mass of Feed Material (100g)] \* 100%

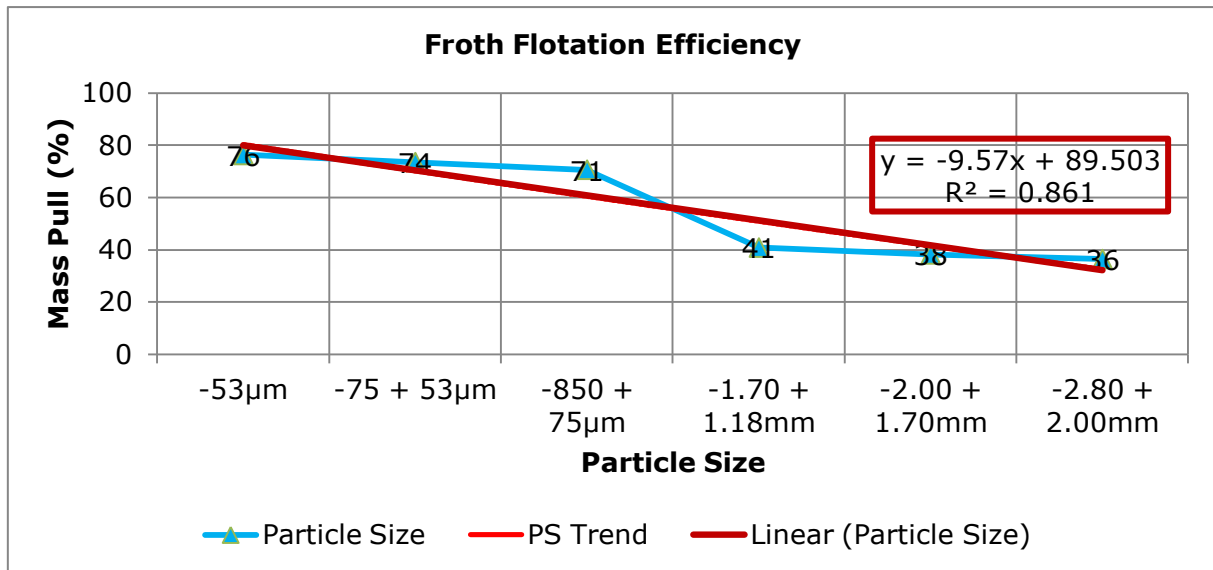


Figure 17: Froth flotation efficiency.

The general trend observed, as supported by the results from the characterisation tests, was that independent from the Collector used, smaller particles from Sample B size fractions demonstrated much higher mass pulls than larger particles from Sample A size fractions. This is because within the same size fraction, carbon will weigh less than grit as grit is more coarse and dense. Therefore from theory, carbon having a lower SG than grit will evidently float but the smaller the carbon, the higher the flotation yield. The opposite remains true for larger sized carbon particles.

#### 4.2.1.1 Statistical Model Analysis

A Statistical Model analysis was performed in order to establish the relationship and use it to make future predictions. It was obtained from the trend line shown on graph relating froth flotation efficiency and particle size and was found to be –

$$y = -9.57x + 89.503 ; \text{ where } R^2 = 0.861 \quad \text{Eq. 12}$$

Based on the statistical regression model, there appears to be a linear relationship between particle size and froth flotation efficiency. The negative slope coefficient of -9.57 suggests that as particle size increases, froth flotation efficiency decreases. In other words, smaller size fractions are more optimally floated than larger size fractions. The  $R^2$  value of 0.861 shows that the model provides a reasonable good fit

to the data, which can be extrapolated to a strong correlation between the two variables and can be reliably predicted using this linear regression model.

Therefore, this model can be used to estimate the froth flotation efficiency of carbon particles based on their size, which could be useful in specific optimisation problems incurred in separating carbon-grit through froth flotation processes at Plant scale.

#### 4.2.2 Effect of Collector-Frother Combination on Mass Pull

To measure the effectiveness that specific reagent combinations have on the floatability of carbon from grit, their effectiveness was quantified using the principle of Mass Pull Frequency<sup>14</sup> on a case by case basis, as shown in Appendix B-3. The relationship between froth flotation efficiency and collector-frother (C-F) combination performance is indicated in the graph below:

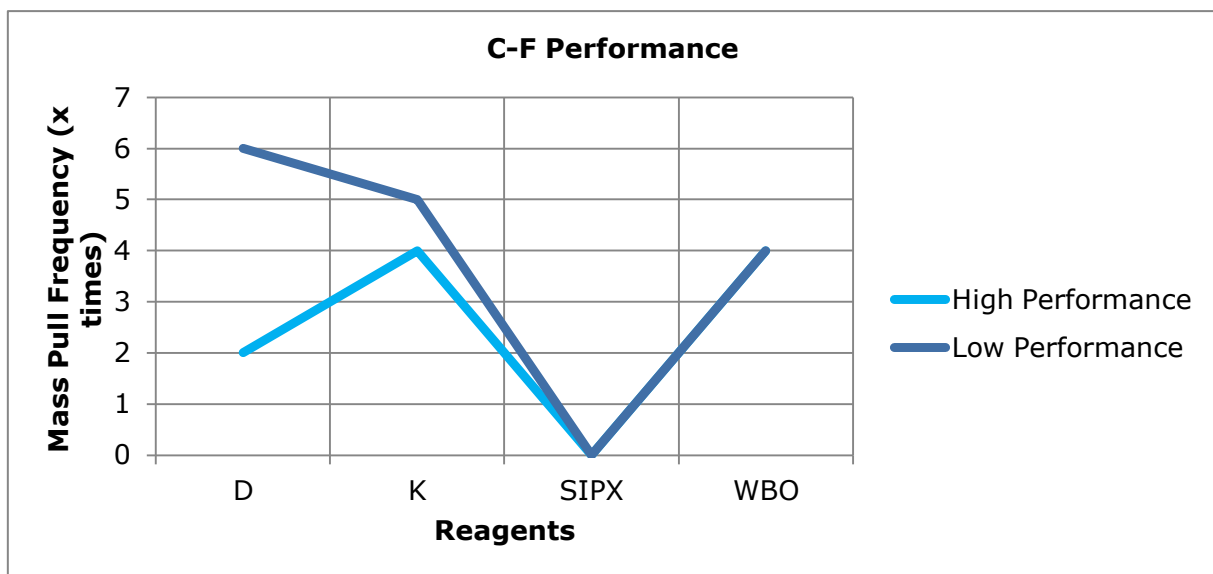


Figure 18: C-F performance per reagent combination basis.

<sup>14</sup> Mass Pull Frequency simply refers to a statistical analysis of the number of times a reagent appeared in a collector-frother combination that was either attributed towards High Performance mass pulls or Low Performance mass pulls. Therefore, 80th percentile mass pull frequency = “high performance” combination. 20th percentile mass pull frequency = “low performance” combination.

The data shows that among the three collectors, Kerosene champions as the best collector in carbon-grit froth flotation, appearing 4 times in combination as a high performance C-F reagent and 5 times in combination for low performance C-F reagent. Diesel comes in second, appearing 2 times and 6 times, respectively. SIPX did not appear in either of the high or low performing C-F combinations, due to lack of discernible impact. This suggests that SIPX may have been of middling effectiveness due to the monolithic nature of each species present at this combination, thereby exhibiting a counter-negative effect at play. This best describes the mediocre flotation yields observed with SIPX.

Waste bio-oil appeared both 4 times in combination as a high performance C-F reagent and 4 times in combination for low performance C-F reagent. Since it was the only frother reagent used for this research, its effectiveness lacks a comparability measure to draw a conclusive deduction from.

#### 4.2.3 Effect of Froth Flotation on Gold Department

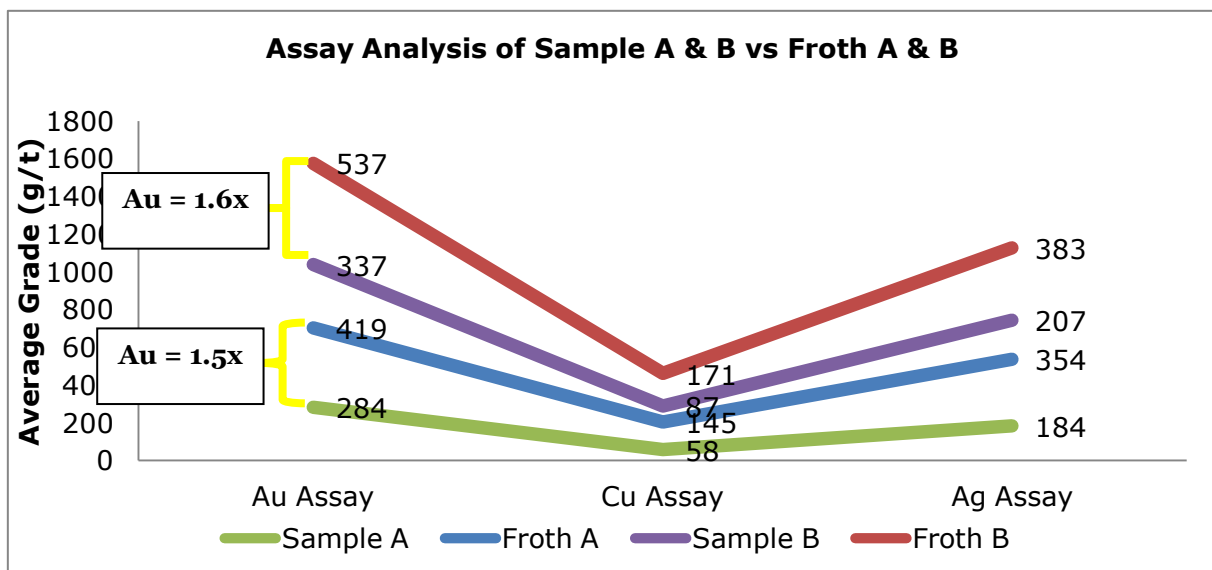


Figure 19 Effect of froth flotation on gold department.

A composite of carbon concentrate A was obtained from mixing the three size fractions under “Sample A”<sup>15</sup> and similarly, a composite of carbon concentrate B was obtained from mixing the three size fractions under “Sample B”<sup>16</sup>, in order to

<sup>15</sup> Sample A = [-2.80mm+2.00mm ; -2.00mm+1.70mm ; -1.70mm+1.18mm]

<sup>16</sup> Sample B = [-1.18mm+850µm ; +850µm-75µm ; -850µm+53µm]

investigate if froth flotation had any notable effect on the initial gold department of the loaded carbon samples.

Comparison made between Sample A composite head assay and Froth A carbon concentrate composite assay showed that Au content increased 1.5 fold from an average of 284g/t to 419g/t, while Sample B composite head assay and Froth B carbon concentrate composite assay showed that Au content increased 1.6 fold from an average of 337g/t to 537g/t. Cu content increased by an average of 2.2 fold while Ag content increased by an average of 1.9 fold, respectively. This is as a result of the concentrating effect of froth flotation, as more loaded carbon reports in the concentrate formed.

Investigating the direct effects that individual flotation reagents used can sequentially have on the dissolution of the gold cyanide complex into solution or the thermodynamics associated with re-adsorption of either fine native gold particles or re-dissolved gold cyanide ions during froth flotation, was beyond the scope of this study due to time and equipment constraints.

### **4.3 Ultrasonic Elution of Loaded Carbon Concentrate**

A carbon concentrate composite<sup>17</sup>, at an average head grade of 478g/t, was considered an “input object” and eluted in a simulation of an elution column fitted with an ultrasonic elution bath. Elution efficiency was estimated by quantifying expected gold dissolution.

The amount of gold present per 1 tonne capacity of feed (loaded carbon) was calculated through the following:

$$\text{Mass of Au per tonne of Carbon (oz)} = [\text{Au Assay (g/t)} * 1\text{t}] / 31.103 \quad \text{Eq. 13}$$

$$\text{Au per tonne of Feed (US\$)} = \text{Mass of Au per tonne of Feed (oz)} * \text{US\$2,039.14/oz}^{18} \quad \text{Eq. 14}$$

---

<sup>17</sup> Froth A and Froth B obtained from previous froth flotation were combined thoroughly to make one carbon froth concentrate. Therefore, composite of loaded carbon can be considered as the material input into the ultrasonic elution step.

<sup>18</sup> Gold price was US\$2,039.14/oz as at 04-May-2023.

Table 3: Expected Gold Sales Value from Processing Loaded Carbon

Sample	Au Assay (g/t)	Au in 1t Feed (oz)	@90% Elution <sup>19</sup> Efficiency (oz)	Au Content (US\$)
Loaded Carbon	478.00	15.368	13.832	28,204.36

In order to justify the expected gold recoveries as shown above, simulation model and sequential mathematical modeling opted to investigate the kinetics, which thereby determine the effectiveness, if any, of ultrasound integration into CASE STUDY’s current elution circuit. The simulation flowsheet is as shown below:

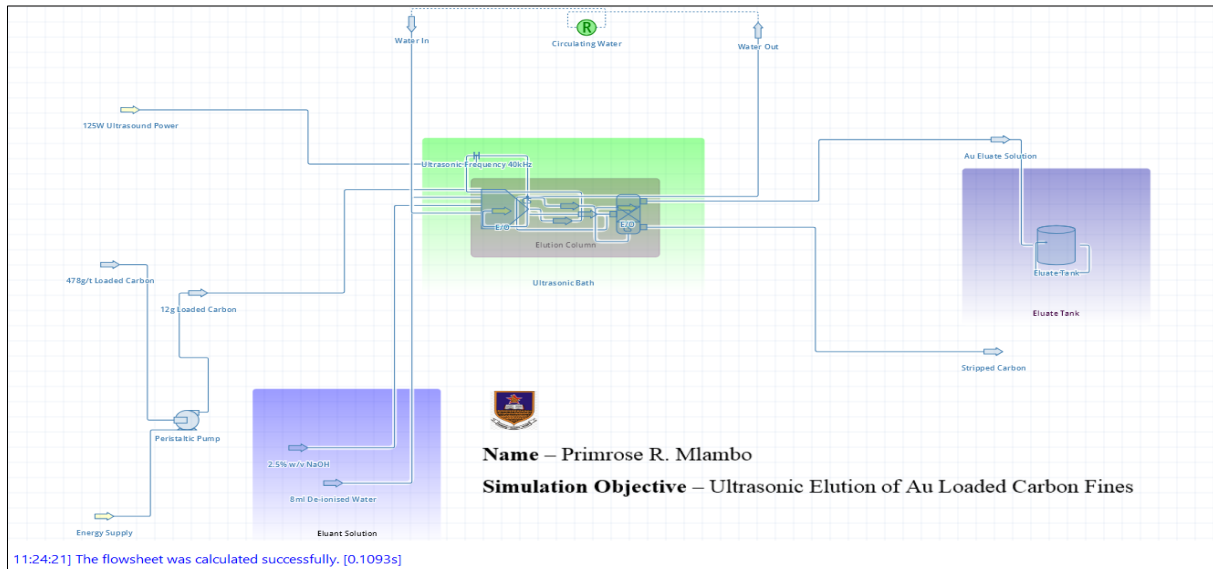


Figure 20: Ultrasonic simulation flowsheet in DWSIM.

### 4.3.1 Steady-State & Elution Efficiency

The simulation flowsheet, based on Raoult’s Law<sup>20</sup>, competently achieved steady-state<sup>21</sup> ultrasonic elution at the following parameters (and at the other parameters noted in Appendix C-1):

<sup>19</sup> CASE STUDY Processing Plant operates at 90% elution efficiency. Source: Historical Data.

<sup>20</sup> Raoult’s Law states that “vapour pressure of an ideal solution is proportional to the mole fraction of each component within the solution”.

<sup>21</sup> Steady-state implies that the simulation has stabilized and is producing constant output that does not change with time or input variations. It is said that the dynamic system is in “an unchanging equilibrium”.

1. [478g/t Loaded Carbon] - Temperature = 25°C, f = 40kHz, Pressure = 101kPa,  
Mass Flow = 1,000kg/h, Molar Flow = 6.48kmol/h

2. [478g/t Eluate] - Temperature = 84°C, frequency = 40kHz, Pressure = 101kPa,  
Mass Flow = 44kg/h, Molar Flow = 3.32kmol/h

From this data, elution efficiency can therefore be theoretically calculated based on either mass flow, 4.4% or on molar flow, 51.2%. These figures provide a good enough framework that can be improved upon, with the goal of obtaining a more efficient steady process flow, due to the less extreme elution parameters conjectured by the presence of an element producing ultrasonic wave energy at a frequency of 40kHz. AARL elution parameters at CASE STUDY require a temperature of 127°C at a pressure of 300kPa, comparable with the realised simulation parameters of operating temperature 84°C and a required operating pressure of 101kPa, again, in order to achieve a stable process flow.

#### 4.3.2 Mathematical Model Analyses of Ultrasonic Elution

##### Universal Base Assumptions

1. Elution is a first-order reaction with respect to  $C_{(s)}[Au]$

$$\therefore \frac{\delta E}{\delta t} \propto C_{(s)}[Au] \quad \text{Eq. 15}$$

2. No Mass Transfer resistance

$$\therefore e_{(aq)}[Au] \leftrightarrow C_{(s)}[Au] \quad \text{Eq. 16}$$

3. Elution is homogenous chemical reaction.

4. Ultrasonic wave energy enhancing elution kinetics.

5. System is under steady-state conditions.

6. Model does not account for external factors affecting elution e.g. changes in pH, flowrate, etc.

7. Model may not be applicable to all systems and requires further validation through experimental data analysis.

## 1. Steady-State Model

### Changes in $e_{(aq)}[Au]$ over Time

#### 1. Mass balance for $C_{(s)}[Au]$

$$\frac{\delta(M_c \cdot C_c)}{\delta t} = -kM_c C_c \quad \text{Eq. 17}$$

#### 2. Mass balance for $e_{(aq)}[Au]$

$$\frac{\delta(M_e \cdot C_e)}{\delta t} = kM_c C_c \quad \text{Eq. 18}$$

#### 3. Energy balance for ultrasonic bath

$$Pt = mc_p \delta T \quad \text{Eq. 19}$$

where:

P - ultrasonic bath power

t - total elution time

$M_e$  - mass of eluant

$c_p$  - specific heat capacity of eluant

$\delta T$  - change in temperature of eluant

#### 4. Energy balance for system

$$Q_{in} - Q_{out} - Q_{loss} = 0 \quad \text{Eq. 20}$$

where:

$Q_{in}$  - input heat energy from ultrasonic bath

$Q_{out}$  - output heat energy from the eluant

$Q_{loss}$  - heat loss from system

## 5. Relationship between input and output rates of mass and energy

$$Q_{in} = P * V \quad \text{Eq. 21}$$

$$M_e = \rho * V \quad \text{Eq. 22}$$

where :

P - ultrasonic bath power

V - volume of eluant

$\rho$  - density of eluant

input and output rates of mass and energy assumed constant

## 6. Rate constant

$$k = AP^B \quad \text{Eq. 23}$$

where:

A and B - constants depending on system parameters in practical conditions

## 7. Change in $e_{(aq)}[\text{Au}]$ over time

$$t = -\ln \frac{\left(\frac{C_e}{C_c}\right)}{k} \quad \text{Eq. 24}$$

## 8 (a) Change in $e_{(aq)}[\text{Au}]$ over time<sup>22</sup>

$$\frac{\delta C_e}{\delta t} = \left[ k * M_c * C_c - C_e * \left( \frac{Q_{out}}{V} \right) \right] / M_e \quad \text{Eq. 25}$$

---

<sup>22</sup> Describes change of gold concentration in eluant solution over time.

## (b) ODE

i) Discrete Form

$$C_e(t + \Delta t) = C_{e(t)} + \Delta t * \frac{(k * M_c * C_c) - (C_{e(t)} * \frac{Q_{out}}{V})}{M_e} \quad \text{Eq. 26}$$

ii) Numerical solution (which can be obtained using Runge-Kutta Method) describes the concentration of  $C_e$  at each time step with higher accuracy and precision.

- **Model objective** – this Base Model helps to observe, ascertain and forecast the rate of ultrasonic elution and how that changes with time.

## 2. Non-Homogenous Model

### Effect of Particle Size with Changes in $e_{(aq)}[Au]$ over Time

#### 1. Relationship between ultrasonic bath power and particle size distribution of GLCF<sup>23</sup>

$$k = A * P^B * f(D_i) \quad \text{Eq. 27}$$

where:

A and B - constants depending on system parameters in practical conditions.

P - ultrasonic bath power

$D_i$  - diameter of GLCF of size i

$f(D_i)$  - function that describes effect of particle size on rate of elution

#### 2. Change in $e_{(aq)}[Au]$ over time<sup>24</sup>

$$\frac{\delta C_e}{\delta t} = \left(\frac{1}{M_e}\right) * \sum_n^{i=1} [k * D_i^2 * N_i * C_i - C_e \left(\frac{Q_{out}}{V}\right)] \quad \text{Eq. 28}$$

where:

n - number of particle size classes

$Q_{out}$  - output heat energy from eluant

- **Model objective** – this particular model helps to observe, ascertain and forecast the degree to which particle size distribution of input loaded carbon affects the rate of gold concentration and how that changes with time.

---

<sup>23</sup> By using a simplified Population Balance Model.

<sup>24</sup> Changes in distribution of particle sizes affects base model system calibration and accessibility of gold on carbon surface to eluant, hence rate of elution affected.

### 3. Non Steady-State Model

#### Effect of Varying Flowrate on $e_{(aq)}[Au]$ over Time

##### 1. Mass balance equations for $C_{(s)}[Au]$ and $e_{(aq)}[Au]$

$$\frac{\delta(M_c \cdot C_c)}{\delta t} = -kM_c C_c \frac{Q_{in}}{Q_{out}} \quad \text{Eq. 29}$$

$$\frac{\delta(M_e \cdot C_e)}{\delta t} = kM_c C_c \frac{Q_{in}}{Q_{out}} \quad \text{Eq. 30}$$

where:

$Q_{in}$  - input flowrate of eluant

$Q_{out}$  - output flowrate of eluant

$Q_{loss}$  - heat loss from system

input and output rates of mass and energy are no longer assumed constant

##### 2. Modified mass and energy balances using new flowrate values<sup>25</sup>

$$M_e = \rho_e \cdot V_e = Q_{out} \cdot t \quad \text{Eq. 31}$$

$$Q_{in} = Q_{out} \cdot \left[ 1 + (c_{p,e} \cdot \left( \frac{T_i - T_e}{h_e \cdot \rho_e} \right)) \right] \quad \text{Eq. 32}$$

$$Q_{out} = Q_{out} \quad \text{Eq. 33}$$

##### 3 (a) Energy balance equation for system<sup>26</sup>

$$\frac{\delta(M_e \cdot C_e \cdot h_e)}{\delta t} = Q_{in} \cdot \left[ 1 - c_{p,e} \left( \frac{T_i - T_e}{h_e \cdot \rho_e} \right) \right] - Q_{out} \cdot \left[ 1 + c_{p,e} \left( \frac{T_e - T_o}{h_e \cdot \rho_e} \right) \right] \quad \text{Eq. 34}$$

where:

<sup>25</sup> How energy in system changes, based on whether laminar, turbulent or composite flow regime.

<sup>26</sup> Note energy changes due to change in temperature of system.

$c_{p,e}$  - specific heat capacity of eluant

$\rho_e$  - density of eluant

$T_i, T_e$  and  $T_o$  - inlet, intermediate and outlet temperatures of eluant

$c_{p,e} * \left( \frac{T_i - T_e}{h_e * \rho_e} \right)$  - shows change in enthalpy of eluant due to  $\delta T$

$c_{p,e} * \left( \frac{T_e - T_o}{h_e * \rho_e} \right)$  - shows change in enthalpy of eluant due to  $\delta P$

## (b) ODE

i) Discrete Form

$$h_{\{n+1\}} = h_n + dt * \left( Q_{in} * \left[ 1 - c_{(p,e)} \frac{(T_i - T_n)}{(h_n * \rho_e)} \right] - Q_{out} * \left[ 1 + c_{(p,e)} \frac{(T_n - T_o)}{(h_n * \rho_e)} \right] \right) / (M_e * C_e) \quad \text{Eq. 35}$$

ii) Numerical solution (which can be obtained using Runge-Kutta Method) will require a weighted average of different slopes in order to compute the value of  $h_{\{n+1\}}$  from  $h_{\{n\}}$

- **Model objective** – this particular model helps to observe, ascertain and forecast how flow regime within elution column affects the rate of gold concentration and how that changes with time.

#### 4. Non Steady-State Model

##### Effect of Varying Frequency on $e_{(aq)}[Au]$ over Time

###### 1. Relationship between input and output rates of heat<sup>27</sup>

$$Q_{in} = U * A * (T_i - T_e) \quad \text{Eq. 36}$$

$$Q_{out} = U * A * (T_e - T_o) \quad \text{Eq. 37}$$

where:

U - overall heat transfer coefficient

A - heat transfer area

$T_i, T_e$  and  $T_o$  - inlet, intermediate and outlet temperatures of eluant

###### 2. Relationship between enthalpy of eluant to its temperature<sup>28</sup>

$$h_e = C_{p,e} * M_e * (T_e - T_{ref}) \quad \text{Eq. 38}$$

where:

$C_{p,e}$  - specific heat capacity of eluant

$M_e$  - mass of the eluant

$T_{ref}$  - reference temperature

- **Model objective** – this particular model helps to observe, ascertain and forecast how changes in ultrasonic frequency range will affect system's thermodynamic stability and the link between rate of gold concentration during elution and how that changes with time.

---

<sup>27</sup> Consider internal energy of the system as ultrasonic waves impart energy to eluant solution molecules.

<sup>28</sup> Observe break-even of optimum thermodynamic stability and kinetics of system.

## **CHAPTER FIVE: CONCLUSION AND RECOMMENDATIONS**

### **5.0 Introduction**

This chapter provides a summary of key findings and hypotheses drawn from the previous four chapters, serving to draw logical conclusions and actionable recommendations from the addressed research aims.

### **5.1 Conclusions**

Following lab scale experimental analysis, the following conclusions were drawn:

1. CASE STUDY is holding a 72t inventory of loaded carbon-grit that will continue to increase due to inevitable carbon losses through continuous CIP/CIL activities.
2. Wilfley Shaking table is operating at a capacity of 6t against a monthly production rate of 7.9t of carbon-grit.
3. Besides pre-existing process inefficiencies that result from eluting smaller size fractions of loaded carbon (< 3mm) in standard AARL parameters, elution circuit is operating at maximum capacity of 42 elution cycles per month, hence Plant cannot halt upstream processes to elute current inventory as plant processing activities are continuous.
4. Froth flotation was successfully able to separate and concentrate loaded carbon from carbon-grit and this phenomena increased the Au assay grade by nearly half, from an average of 311g/t to 478g/t.
5. Smaller size fractions (<850µm) produced the highest froth flotation yields.
6. Kerosene and Waste Bio-Oil combination showed excellent selectivity, as 100% of the froth concentrate composition was made of carbon, with no problem of entrapment of unwanted material reporting in the froth concentrate.
7. Flotation cell ran for a cumulative of 30 minutes to obtain maximum flotation yields.
8. Among the three collectors tested, Kerosene within the range of 0.3-0.6% TV in combination with Waste Bio-Oil within the range of 0.3-0.6% TV produced the highest mass pulls, within the upper 80<sup>th</sup> percentile.

9. Elution simulation achieved steady-state at 84 °C and 101kPa, which is 43 °C less and 199kPa less than current operational parameters.
10. Based on mass flow, simulation ultrasonic elution efficiency achieved was 4.4%.
11. However, based on molar flow, simulation ultrasonic elution efficiency achieved was 51.2%.
12. Mathematical modeling framework that analyses ultrasonic elution efficiency at steady-state, non-steady-state and non-homogenous conditions, has been laid out.
13. Four mathematical models observe how gold concentration over time is affected by particle size distribution, flow regime and the thermodynamic variations imposed by an altering ultrasonic frequency.
14. 1t of loaded carbon of average head grade 478g/t at CASE STUDY's current 90% elution efficiency is equivalent to a monetary value of US\$28,204.36.<sup>29</sup>
15. CASE STUDY currently runs 6t of loaded carbon in 1 elution, completing a total of 42 elutions per month means an annual revenue boost of US\$7,107,498.72 from ultrasonic-based elution.
16. As stated in Chapter 2, an untapped market of between 500,000-1,500,000 artisanal gold miners exists in Zimbabwe.<sup>30</sup>
17. CASE STUDY can purchase artisanal gold miners' loaded carbon fines, which they cannot elute in the commonly employed "boiler mechanism", hence is considered waste material to them.
18. Overall, this research project proves to be a lucrative and marginal source of revenue, into the foreseeable future of gold processing at CASE STUDY, minimising gold lockup in carbon-grit inventory.

## 5.2 Recommendations

Aforementioned conclusions of this research project came about with experimental limitations that must be taken into consideration, prior to plant scale adaptation of froth flotation and ultrasonic-based model of processing carbon-grit. Factors affecting said aims were wide and inexhaustible to investigate experimentally either through lab scale techniques or mathematical models, hence the scope of this

---

<sup>29</sup> Calculated based on gold price as at 04-May-2023 of US\$2,039.14/oz.

<sup>30</sup> Zimbabwe Miners Federation. (2019). About us. Retrieved from <https://www.zmf.org.zw/about>

research project is limited. It is therefore, my recommendation that further lab scale experimentation should be done to observe the direct effects of –

- Varying % TV of collector or frother added.
- Single acting reagents on froth flotation yield.
- Reusing flotation reagents and process water mixture.
- Flotation reagents on gold dissolution during the froth flotation process.
- Using alternative collectors, e.g. oleic acid, dodecylamine and frothers, e.g. methyl isobutyl carbinol (MIBC), Downfroth™, to mention a few.
- Varying ultrasonic frequency within the range of 20kHz to 60kHz, in a variable non-static simulation model.
- Pilot plant froth flotation tests.
- Lab scale ultrasonic elution tests.

### **5.2.1 Validation of Mathematical Models**

To identify any discrepancies or limitations caused by model assumptions, validation of the proposed mathematical models from Chapter 4 can be done through lab scale tests (highlighted in Chapter 3) focused on the following three aspects –

1. Mass transfer
  2. Elution kinetics
  3. Ultrasonic wave energy
- 
- Proposed flowsheet for the ultrasonic elution plant set up is as shown in Chapter 4, Figure 20.

# Bibliography

1. Achaw, O. W. & Danso-Boateng, E., 2021. Equilibrium isotherms and thermodynamic properties of gold adsorption onto activated carbon. *Journal of Materials Research and Technology*, 10(1), pp. 128-141.
2. Adam, K., 1994. Elution of gold from carbon by the micron solvent distillation procedure. *Hydrometallurgy*, 35(1), pp. 107-119.
3. Adams, M. D., 2016. *Gold Ore Processing: Project Development and Operations*. s.l.:Elsevier Inc.
4. Barbian, N., Prinsloo, A. & Aldrich, C., 2019. A review of froth flotation control. *International Journal of Mineral Processing*, 187(1), pp. 107-121.
5. Breitbach, Z. S., Miller, J. D. & Dyer, R. B., 2003. Enhanced desorption of organic pollutants from soils using ultrasonic irradiation. *Environmental Science & Technology*, 37(4), pp. 832-838.
6. Chen, X., Gao, X. & Li, G., 2019. Flotation separation of carbon fines from fly ash using a surfactant. *Separation and Purification Technology*, 215(1), pp. 128-134.
7. Chiririwa, H. & al, e., 2016. The influence of ultrasonic waves on the elution of platinum and gold from activated carbon. *Ultrasonics Sonochemistry*, 33(1), pp. 142-148.
8. Coetzee, L. C. & Cloete, T. E., 1998. The effect of impeller type on the breakage of activated carbon.. *Hydrometallurgy*, 23(2), pp. 209-218.
9. Elias, G. & Martínez, J., 2019. Simulation of the adsorption of metal ions on activated carbon using DWSIM. *Chemical Engineering Education*, 53(3), pp. 137-144.
10. Feng, D., Aldrich, C. & Senanayake, G., 2003. A comparison of laboratory and pilot plant scale of ultrasonic enhanced elution of gold from activated carbon. *Minerals Engineering*, 16(10), pp. 961-966.
11. Fleming, C. A. & Cromberge, G., 1984. The Effect of Particle Size on the Rate of Gold Desorption from Activated Carbon. *Canadian Metallurgical Quarterly*, Volume Canadian Metallurgical Quarterly, 23(4), p. 363-366., pp. 363-366.
12. FRGM, n.d. *Carbon fines in gold recovery*. [Online] Available at: <https://frgminerals.com/carbon-fines-in-gold-recovery> [Accessed 25 April 2023].

13. Fuerstenau, D. W., 1983. *Coal Surface Chemistry and Flotation Behavior*. s.l.:s.n.
14. Fuerstenau, M. C., Jameson, G. J. & Yoon, R. H., 2007. *Froth flotation: A century of innovation*. s.l.:Society for Mining, Metallurgy and Exploration Inc..
15. Gama, F., Braga, T. & Rubio, J., 2020. The Effect of Bio-Oil as a Frother in Column Flotation of Coal. *Energies*, 13(24), p. 6688.
16. Gao, R. & Liu, J., 2018. The Role of Sodium Metabisulfite in the Flotation Separation of Copper–Molybdenum Sulfides. *Minerals*, 8(11), p. 498.
17. Gao, X., Chen, X. & Li, G., 2018. Microwave augmented ashing for carbonaceous fines recovery from a waste residue. *Separation and Purification Technology* 194, 194(1), pp. 401-406.
18. Gao, X., Chen, X. & Li, G., 2020. Application of machine learning algorithms in mineral flotation: A review. *Minerals Engineering*, 106065(1), p. 147.
19. Gerson, A. R. & Klemm, W., 1990. Uses of organic reagents in flotation of carbonaceous and sulfide ores. In: A. V. Nguyen & S. K. Kawatra, eds. *Flotation reagents: Applied surface chemistry on minerals flotation and energy resources beneficiation*. s.l.:Society for Mining, Metallurgy and Exploration Inc., pp. 117-134.
20. Gupta, R. P., n.d. In: *Coal Flotation and Fine Coal Utilization*. s.l.:Elsevier Science Publishers, pp. 1-32.
21. Habashi, F., 1999. *A Textbook of Hydrometallurgy*. 1 ed. Quebec: Métallurgie Extractive Québec.
22. Habashi, F., 2015. *Handbook of extractive metallurgy*. 1 ed. s.l.:Wiley-VCH.
23. Hamdaoui, O., Chiha, M. & Naffrechoux, E., 2005. Elaboration of a novel ultrasound-assisted method for the desorption of heavy metals from activated carbon. *Ultrasonics Sonochemistry*, 12(5), pp. 367-372.
24. Hassler, J. W., 1974. Activated carbon. *Chemical Reviews*, 74(3), pp. 201-217.
25. He, Y. B. & Laskowski, J. S., 1992. Role of surface forces in flotation of fine coals. *Colloids and Surfaces*, 64(1), pp. 93-104.
26. Hilson, G. & Murck, B., 2007. Sustainability, gold mining, and the development of a gold mining sustainability scorecard. In: E. L. Brown, ed. *Handbook of Gold Exploration and Evaluation*. Colorado: Society of Mining, Metallurgy and Exploration Inc..

27. Hove, E., 2021. *Kuvimba in historic 300kg gold haul. The Herald Business Reporter*. [Interview] (17 June 2021).
28. Jolly, A. & al., e., 2014. Optimisation of ultrasonic-assisted elution of gold from loaded activated carbon. *Minerals Engineering*, 65(1), pp. 16-23.
29. Kawatra, S. K., Ripke, S. J. & Dwari, R. V., 2021. Reusing mine water in mineral processing. *Minerals Engineering*, 106845(1), p. 163.
30. Kitchener, J. A., Boxall, J. A. & Arya, S. K., 2019. Green surfactants for mineral flotation: A review on their synthesis, properties and applications. *Minerals Engineering*, 134(1), pp. 20-29.
31. Lee, J. H., Park, S. W. & Seo, Y. C., 2012. Environmentally friendly recovery of coal fines using waste oil. *Journal of Hazardous Materials*, 1(1), pp. 227-228, 491-496.
32. Liu, Y., Li, D., Zhang, W. & Chen, X., 2020. Optimization of flotation process for coal fines using a machine learning algorithm. *Minerals Engineering*, 106072(1), p. 147.
33. Li, Y., Liu, J., Xiong, Y. & Xing, Y., 2021. A machine learning-based approach for predicting flotation recovery of scheelite minerals. *Minerals Engineering*, 106757(1), p. 166.
34. Maitson, A. T. & Mark, H. B., 1971. Adsorption. In: *In Encyclopaedia of Chemical Technology 2(1)*. s.l.:Wiley-Interscience, pp. 347-390.
35. Manrique, O. A. & al., e., 2019 . *Mathematical modeling of gold elution from activated carbon using Euler's method*. s.l., s.n., p. 12032.
36. Marsden, J. O. & House, I. C., 2006. *The chemistry of gold extraction*. 1 ed. Colorado: SME, Littleton.
37. Moyo, S. & al., e., 2015. Modeling of the carbon in pulp (CIP) process in gold cyanide leaching plants using the plant data. *Minerals Engineering*, 83(1), pp. 88-96.
38. Murinda, S. E. & al, e., 2018. Mathematical modelling of ultrasonic-assisted gold desorption from activated carbon. *Journal of the Southern African Institute of Mining and Metallurgy*, 118(7), pp. 739-746.
39. Peng, Y. & Zhao, Y., 2019. Study on the flotation behavior of carbon fines with kerosene as collector. *Energy Sources, Part A: Recovery, Utilization, and Environmental Effects*, 41(14), pp. 1754-1764.
40. Rao, K., Iyengar, L. & Rao, K., 2008. Elution and Regeneration of Activated Carbon. *Journal of Chemical Sciences*, 120(2), pp. 203-211.

41. Rogans, J., n.d. *Activated Carbon*. Johannesburg: Kemix Pty Ltd.
42. Rowe, C. A. & McKnight, S., 2009. The management of activated carbon in gold recovery circuits. *Journal of Cleaner Production*, 17(16), pp. 1433-1444.
43. Sivamohan, R. & Forsberg, E., 1985. Principles of tabling. *International Journal of Mineral Processing*, 15(4), p. 2.
44. Smith, J., 2023. *Benefits of using DWSIM over METSIM for ultrasonic elution of carbon fines*. [Online] Available at: <https://www.example.com/benefits-of-using-dwsim-over-metsim> [Accessed 26 April 2023].
45. Somasundaran, P. & Harris, C. C., 1982. Role of kerosene in flotation separation of quartz from feldspar. *Transactions of the Indian Institute of Metals*, 35(4), pp. 61-365.
46. Strudgeon, G. A. & al., e., 1980. Regeneration of activated carbon used for recovery of gold. *Canadian Journal of Chemical Engineering*, 58(4), pp. 417-422.
47. Sun, Z. & Pan, J., 2018. A review of oil agglomeration techniques for fine mineral recovery. *Minerals Engineering*, 120(1), pp. 129-137.
48. Tiernon, J., 1973. *Physical coal cleaning*, s.l.: US Department of Energy.
49. Van Dam, J. A., 1994. Adsorption of gold from pulp by activated carbon. *Minerals Engineering*, 7(12), pp. 1463-1483.
50. Wang, Y. & al., e., 2020. Mathematical modeling of ultrasonic-assisted desorption of gold from activated carbon. *Ultrasonics Sonochemistry*, 63(1), p. 104928.
51. Yu, L., Yu, W., Zhou, Y. & Zhang, D., 2003. Study on the desorption of gold from activated carbon using mixed solvents of ethanol and sodium hydroxide. *Journal of Central South University of Technology*, 10(2), pp. 97-101.
52. Zhang, J. & Wang, Y., 2019. A review of the beneficiation of rare earth element bearing minerals by flotation. *Reviews in Chemical Engineering*, 35(6), pp. 777-787.
53. Zhang, M., Liu, X., Liu, G. & Wang, X., 2019. Beneficiation of low-grade coal fines using a novel enhanced gravity separator. *Fuel*, 240(1), pp. 146-151.
54. Zhang, T., Chen, X. & Yin, W., 2021. Ultrasonic-assisted elution of gold from activated carbon: A review. *Ultrasonics Sonochemistry*, 73(1), p. 105477.

55. Zhang, Y. & Li, J., 2013 . Mathematical model for ultrasonic-assisted elution of gold from activated carbon. *Journal of the Southern African Institute of Mining and Metallurgy*, 113(11), pp. 863-868.
56. Zhao, L., Li, X., Peng, Y. & Liu, J., 2021. Application of Waste Bio-Oil as a Novel Frother in Flotation Separation of Graphite. *Minerals*, 11(4), p. 355.
57. Zimmerman, J. B., 1981. Coal preparation plant advances. *Mining Engineering*, 33(6), pp. 651-657.
58. Zimmerman, J. B., 1982. Coal preparation plant advancements in the United States. *International Journal of Mineral Processing*, 9(1), pp. 1-16.

# Appendices

## Appendix A: Characterisation Results

### 1. Wilfley Table Analyses

	High Recovery Ratio Mining Wilfley Table
Model Number	LY4500
Certification	ISO9001:2008
Warranty	1-Year
Material	High Carbon Steel
Voltage	380V
Weight	< 1t
Wilfley Table Capacity	2.31x10 <sup>-6</sup> t/s or 0.200t/day
C-G Inventory as at February 2022	72t
Tank Sanding Rate	1 tank/month
Average Mass of Carbon in One CIL Tank per Month	1.710t
Mass of Carbon from One Sanded Tank per Month	1.710t
Abrasion Rate of Donau 6x12	3.7%/1t of Activated Carbon
Mass of Carbon Fines per Tank per Month	0.026t
Mass of Carbon Fines in CIL per Month	0.182t
Mass of Escaped Carbon at Tailings Section per Day	0.200t
Mass of Escaped Carbon at Tailings Section per Month	6t
Total Mass of Unprocessed C-G Produced per Month	7.892t
Wilfley Table Capacity per Month	6t
Time Taken to Process 72t Inventory	12 months
In 12 months, Unprocessed C-G Produced	94.704t
Time Taken to Process 94.704t Inventory	15 months
In 15 months, Unprocessed C-G Produced	118.380t
Time Taken to Process 118.380t Inventory	19 month
In 19 month, Unprocessed C-G Produced	149.948t
Time Taken to Process 149.948t Inventory	24 months
	and so on...

## 2. Abrasion Test Results

Control Donau 6x12 Abrasion Rate = 3.70%

Conditioning weight = weight of carbon retained by screen

True weight = weight of carbon retained by screen

	Test	Sample Weight (g)	True Weight (g)	Conditioning Weight (g)	Abrasion Rate (%)
Control	1	30	27.94	26.87	3.57
	2	30	28.88	27.75	3.77
	3	30	27.99	26.89	3.67
				Average Abrasion Rate (%)	3.67
Sample A	1	30	28.99	28.50	1.63
	2	30	27.86	27.43	1.43
	3	30	27.94	27.61	1.10
				Average Abrasion Rate (%)	1.39
Sample B	1	30	29.91	29.77	0.47
	2	30	28.87	28.56	1.03
	3	30	28.92	28.85	0.23
				Average Abrasion Rate (%)	0.58

## 3. Specific Gravity Test Results

	Test	Mass (g)	Volume (ml)	SG	
Control	1	70	120	0.58	
Most C between 3.35mm - 2.80mm	2	100	169	0.59	
	3	250	421	0.59	
				Average SG	0.59
Sample A	1	70	78	0.90	
95% C between 2.00mm - 1.18mm	2	100	110	0.91	
	3	250	274	0.91	
				Average SG	0.91
Sample B	1	70	188	0.37	
60% C between 850µm - 75µm	2	100	245	0.41	
	3	250	551	0.45	
				Average SG	0.41

#### 4. Carbon-grit PSD - Au, Ag,Cu Department

Sample A	Aperture (mm)	Mass Retained (g)	Carbon Composition (%)	G Composition (%)	Au Assay (g/t)
	4.75	49.00	0	100	n/a
	3.35	54.00	0	100	n/a
	2.80	40.00	50	50	216
	2.00	256.00	80	20	301
	1.70	177.00	95	5	338
	1.18	379.00	90	10	325
	850.00	344.00	65	35	244
	-850.00	301.00	30	70	261
		1600.00			

Sample B	Aperture (µm)	Mass Retained (g)	Carbon Composition (%)	G Composition (%)	Au Assay (g/t)
	850.00	307.00	40	60	340
	75.00	822.00	60	40	345
	53.00	471.00	15	85	326
		1600.00			

### Appendix B: Froth Flotation Results

#### 1. Mass Pull (%) – Rougher-Cleaner Stage

t = 30 minutes	Sample A			Sample B			
	C-F Combination	- 2.80+2.00 mm	-2.00 + 1.70mm	-1.70 + 1.18mm	-850+75 µm	-75 + 53µm	- 53µm
	K + S	44.00	44.00	49.00	81.00	80.00	86.00
	D + S	46.00	47.00	45.00	79.00	80.00	82.00
	K + D + S	37.00	39.00	40.00	77.00	77.00	79.00
	K + WBO	46.00	49.00	52.00	85.00	86.00	89.00
	D + WBO	45.00	48.00	55.00	80.00	83.00	87.00
	K + D + WBO	42.00	48.00	51.00	79.00	80.00	87.00
	S + WBO	45.00	48.00	49.00	70.00	78.00	79.00
	S + WBO + K	44.00	46.00	46.00	70.00	75.00	78.00

S + WBO + D	42.00	43.00	46.00	66.00	72.00	75.00
S + WBO + K + D	36.00	37.00	41.00	62.00	69.00	72.00

## 2. Mass Pull (%) – Rougher-Scavenger Stage

t = 15 minutes	Sample A			Sample B		
C-F Combination	-2.80 + 2.00mm	-2.00 + 1.70mm	-1.70 + 1.18mm	-850 + 75µm	-75 + 53µm	- 53µm
K + S	31.00	36.00	39.00	70.00	73.00	74.00
D + S	30.00	31.00	34.00	64.00	65.00	67.00
K + D + S	28.00	28.00	31.00	57.00	62.00	64.00
K + WBO	34.00	37.00	39.00	76.00	79.00	79.00
D + WBO	32.00	33.00	36.00	75.00	78.00	79.00
K + D + WBO	30.00	32.00	35.00	72.00	73.00	76.00
S + WBO	34.00	34.00	36.00	66.00	67.00	70.00
S + WBO + K	30.00	31.00	33.00	64.00	67.00	70.00
S + WBO + D	29.00	30.00	32.00	60.00	64.00	65.00
S + WBO + K + D	24.00	24.00	28.00	60.00	63.00	68.00

## 3. High Performance & Low Performance Mass Pull Frequency

High Performance	Av. Mass Pull	Mass Pull Frequency
D	87.00	2
K	87.00	4
SIPX	0.00	0
WBO	87.25	4

Low Performance	Av. Mass Pull	Mass Pull Frequency
D	26.83	6
K	26.40	5
SIPX	0.00	0
WBO	26.25	4

## Appendix C: Ultrasonic Elution Simulation Data Set

### 1. Simulation at Steady-State Parameters by Object

Object: 478g/t Loaded Carbon		
Temperature	25	°C
Pressure	1.01325	bar
Mass Flow	1000	kg/h
Molar Flow	6.48034	kmol/h
Volumetric Flow	0.79558	m <sup>3</sup> /h
Density (Mixture)	1256.95	kg/m <sup>3</sup>
Molecular Weight (Mixture)	154.313	kg/kmol
Specific Enthalpy (Mixture)	-5365.19	kJ/kg
Specific Entropy (Mixture)	-17.7453	kJ/[kg.K]
Molar Enthalpy (Mixture)	-827918	kJ/kmol
Molar Entropy (Mixture)	-2738.33	kJ/[kmol.K]
Thermal Conductivity (Mixture)	0.103052	W/[m.K]
Object: Energy Supply		
Energy Flow	0.264803	kW
Object: 12g Loaded Carbon		
Temperature	25.1269	°C
Pressure	10	bar
Mass Flow	1000	kg/h
Molar Flow	6.48034	kmol/h
Volumetric Flow	0.795021	m <sup>3</sup> /h
Density (Mixture)	1257.83	kg/m <sup>3</sup>
Molecular Weight (Mixture)	154.313	kg/kmol
Specific Enthalpy (Mixture)	-5364.24	kJ/kg
Specific Entropy (Mixture)	-17.8578	kJ/[kg.K]
Molar Enthalpy (Mixture)	-827771	kJ/kmol
Molar Entropy (Mixture)	-2755.69	kJ/[kmol.K]
Thermal Conductivity (Mixture)	0.103029	W/[m.K]
Object: 2.5% w/v NaOH		
Temperature	25	°C
Pressure	1.01325	bar
Mass Flow	5.65	kg/h
Molar Flow	0.141261	kmol/h
Volumetric Flow	0.00265258	m <sup>3</sup> /h
Density (Mixture)	2130	kg/m <sup>3</sup>

Molecular Weight (Mixture)	39.997	kg/kmol
Specific Enthalpy (Mixture)	675.532	kJ/kg
Specific Entropy (Mixture)	2.26575	kJ/[kg.K]
Molar Enthalpy (Mixture)	27019.3	kJ/kmol
Molar Entropy (Mixture)	90.6231	kJ/[kmol.K]
Thermal Conductivity (Mixture)	0	W/[m.K]

---

Object: 8ml De-ionised Water

---

Temperature	25	°C
Pressure	1.01325	bar
Mass Flow	20	kg/h
Molar Flow	1.11017	kmol/h
Volumetric Flow	0.0200737	m <sup>3</sup> /h
Density (Mixture)	996.327	kg/m <sup>3</sup>
Molecular Weight (Mixture)	18.0153	kg/kmol
Specific Enthalpy (Mixture)	-2440.95	kJ/kg
Specific Entropy (Mixture)	-8.18698	kJ/[kg.K]
Molar Enthalpy (Mixture)	-43974.4	kJ/kmol
Molar Entropy (Mixture)	-147.491	kJ/[kmol.K]
Thermal Conductivity (Mixture)	0.610248	W/[m.K]

---

Object: Stripped Carbon

---

Temperature	84.6575	°C
Pressure	1.01325	bar
Mass Flow	43.7862	kg/h
Molar Flow	3.31663	kmol/h
Volumetric Flow	0.0243051	m <sup>3</sup> /h
Density (Mixture)	1801.52	kg/m <sup>3</sup>
Molecular Weight (Mixture)	13.202	kg/kmol
Specific Enthalpy (Mixture)	-115946	kJ/kg
Specific Entropy (Mixture)	-323.956	kJ/[kg.K]
Molar Enthalpy (Mixture)	-1.53072E+06	kJ/kmol
Molar Entropy (Mixture)	-4276.87	kJ/[kmol.K]
Thermal Conductivity (Mixture)	2.5162	W/[m.K]

---

Object: Peristaltic Pump

---

Pressure Increase (Head)	8.98675	bar
Efficiency	75	
Temperature Difference	0.12689	°C.
Power Required	0.264803	kW
Available NPSH	8.21137	m
Outlet Pressure	10	bar
Head	72.8815	m

Object: Water In		
Temperature	84.6575	°C
Pressure	1.01325	bar
Mass Flow	5980.12	kg/h
Molar Flow	331.943	kmol/h
Volumetric Flow	6.17396	m <sup>3</sup> /h
Density (Mixture)	968.603	kg/m <sup>3</sup>
Molecular Weight (Mixture)	18.0155	kg/kmol
Specific Enthalpy (Mixture)	-2188.48	kJ/kg
Specific Entropy (Mixture)	-6.087	kJ/[kg.K]
Molar Enthalpy (Mixture)	-39426.4	kJ/kmol
Molar Entropy (Mixture)	-109.66	kJ/[kmol.K]
Thermal Conductivity (Mixture)	0.672744	W/[m.K]
Object: Water Out		
Temperature	84.6575	°C
Pressure	1.01325	bar
Mass Flow	5980.12	kg/h
Molar Flow	331.943	kmol/h
Volumetric Flow	6.17396	m <sup>3</sup> /h
Density (Mixture)	968.603	kg/m <sup>3</sup>
Molecular Weight (Mixture)	18.0155	kg/kmol
Specific Enthalpy (Mixture)	-2188.48	kJ/kg
Specific Entropy (Mixture)	-6.087	kJ/[kg.K]
Molar Enthalpy (Mixture)	-39426.4	kJ/kmol
Molar Entropy (Mixture)	-109.66	kJ/[kmol.K]
Thermal Conductivity (Mixture)	0.672744	W/[m.K]
Object: 125W Ultrasound Power		
Energy Flow	33	kW
Object: Ultrasonic Frequency 40kHz		
Flow Conductance	1	[kg/s]/[Pa <sup>0.5</sup> ]
Volume	1	m <sup>3</sup>
Minimum Pressure	1.01325	bar
Initialize using Inlet Stream	1	
Reset Content	0	
Pressure Drop	0	bar
Efficiency	100	
Outlet Temperature	84.6575	°C

Heat Added	33	kW
Outlet Molar Vapor Fraction	0	
Temperature Difference	4.22792	°C.
<hr/>		
Object: Au Eluate Solution		
<hr/>		
Temperature	84.6575	°C
Pressure	1.01325	bar
Mass Flow	961.864	kg/h
Molar Flow	3.30497	kmol/h
Volumetric Flow	1.07933	m <sup>3</sup> /h
Density (Mixture)	891.17	kg/m <sup>3</sup>
Molecular Weight (Mixture)	291.035	kg/kmol
Specific Enthalpy (Mixture)	-177.502	kJ/kg
Specific Entropy (Mixture)	-0.420402	kJ/[kg.K]
Molar Enthalpy (Mixture)	-51659.5	kJ/kmol
Molar Entropy (Mixture)	-122.352	kJ/[kmol.K]
Thermal Conductivity (Mixture)	0.0811101	W/[m.K]
<hr/>		
Object: Eluate Tank		
<hr/>		
Liquid Level	0	m
Height	2	m
Initialize using Inlet Stream	0	
Reset Content	0	
Pressure Drop	0	bar
Volume	3	m <sup>3</sup>
Residence Time	2.77951	h
<hr/>		

## Appendix D: File Resources

		
MLAMBO_Project_Results.xlsx	MLAMBO_Ultrasonic Elution_Simulation.dwg	MLAMBO_Project_Presentation.pdf